Spring 1-27-1964

Slope Deposits of the Pennsylvanian Haymond Formation, Marathon Region, Texas

Walter E. Dean Jr.

SLOPE DEPOSITS OF THE PENNSYLVANIAN HAYMOND FORMATION · DEAN

NAME AND ADDRESS	DATE
E. F. McBride Dept. Geology Univ Texas	Feb 29 1965
E F McBride Dept. Geology Univ, Texas	May 20, 1965
[illegible] Plano Texas	June 27 1968
C. Tafoya UNM-VC-Tome, NM	29 June 1987

SLOPE DEPOSITS OF THE PENNSYLVANIAN HAYMOND FORMATION, MARATHON REGION, TEXAS

by

Walter E. Dean, Jr.

A Thesis

Submitted in Partial Fulfillment of the

Requirements for the Degree of

Master of Science in Geology

The University of New Mexico

1964

This thesis, directed and approved by the candidate's committee, has been accepted by the Graduate Committee of the University of New Mexico in partial fulfillment of the requirements for the degree of

MASTER OF SCIENCE

W. J. Parish
Dean

Jan. 27, 1964
Date

Thesis committee

Roger Y. Anderson
Chairman

Sherman A. Wengerd

J. Paul Fitzsimmons

321715

CONTENTS

Page

ILLUSTRATIONS

ABSTRACT

The Haymond Formation of the Marathon basin, Texas consists mainly of a sequence of more than 12,000 siltstone-shale couplets which, combined with the similar couplets of the older Tesnus Formation, form a sequence of "flysch" sediments more than 10,000 feet thick deposited on the eastern slope of the subsiding Llanoria geosyncline. The Haymond Formation contains no diagnostic fossils; its age is known only as Lower Pennsylvanian, probably Atokan.

The siltstone and shale of the Haymond Formation differ in the relative amounts of quartz and clay matrix. There are also thin silty claystone layers which are closest to the shales in composition but resemble the siltstone layers in weathering characteristics. The silty claystone is believed to represent the downslope decrease of silt within siltstone layers. The calcium carbonate, magnesium carbonate, iron, and organic (Kjeldahl) nitrogen composition show little or no trends throughout the section.

The siltstone-shale couplets are the most obvious sedimentary structures in the Haymond Formation. The contact between a silt layer and the underlying clay layer is sharp, indicating rapid deposition by a silt-laden current. The gradational contact between the same silt layer and the overlying clay layer indicates a waning of the current and a reduction in the amount of silt, resulting in a sedimentologic silt-clay couplet.

Internal sedimentary structures, accentuated by X-radiographs and hydrofluoric acid etching, include horizontal micro-

The [illegible]

results of a [illegible]

water, [illegible]

formation [illegible]

feet [illegible]

limonite [illegible]

[illegible]

stone.

The [illegible]

in the pelite [illegible]

also thin shiny layer [illegible]

in conformation [illegible]

characteristic [illegible]

the development [illegible]

detrital carbonates, [illegible]

[illegible]

out the section.

The silicon [illegible]

structures in the [illegible]

layer and the [illegible]

formation by [illegible]

between the [illegible]

a weight of the [illegible]

[illegible]

[illegible]

and [illegible]

laminations, cross-laminations, convolute-laminations, and graded bedding. The convolute-laminations are the result of plastic gravity deformation of horizontal or cross laminations in the upper part of silt layers. Vertical graded bedding is rarely noticeable except in the gradational contact between the silt and clay layers. Lateral grading is indicated by a 45 percent increase in thickness and a 46 percent increase in the number of silt layers within 5 miles in an upslope direction. Lateral persistence of the thickest layers is demonstrated by a +0.998 correlation coefficient over the 5 mile interval.

Directional measurements of 357 flute and groove casts on the lower bedding planes of silt layers indicate current azimuths, measured from south, ranging from 55^{0} to 128^{0} with a mean of 85^{0}, implying an eastern source of material.

Thickness variations of the silt-clay couplets appear to be random although zones of thick couplets occur at the bottom and top of the section and exceptionally thick couplets were separated by an average of 40 thinner couplets. Seventy-five percent of all individual silt and clay layers are less than 0.2 foot thick.

The silt layers represent deposition by turbidity currents that were probably triggered by severe storms with an average frequency of less than 5 years. The downslope decrease in couplets indicates that not all of these storms were recorded as silt-clay couplets in the area of study.

INTRODUCTION

Location

The Haymond Formation is exposed in several northeast-trending synclinal valleys in the Marathon basin (Fig. 1). Located in the northern part of Brewster County in the Big Bend region of Texas, the Marathon topographic basin is 40 miles long and 30 miles wide and was formed by the erosion of a broad dome of Cretaceous limestone. The basin is bounded on the east, south, and west by gently dipping Cretaceous limestone and on the north by the Glass Mountains. Within the basin, tightly folded Paleozoic sediments form a series of northeast-trending ridges and valleys. The ridges are formed by the erosion of nonresistant shale enclosing two resistant formations, the Caballos Novaculite (Devonian ?) and the Dimple Limestone (Pennsylvanian). The Haymond Formation overlies the Dimple Limestone and forms several valleys to the east of Dimple ridges. Because of the mantle of alluvium, good exposures of the Haymond Formation are limited to cuts along U. S. Highway 90 and the Southern Pacific Railroad, and occasionally in stream banks. Two exposures of the Haymond Formation were chosen for this study. The first exposure is about 15 miles east of Marathon on U. S. Highway 90. The second exposure is in the type locality of the Haymond Formation about 2 miles east of Haymond station on the Southern Pacific Railroad (Fig. 1).

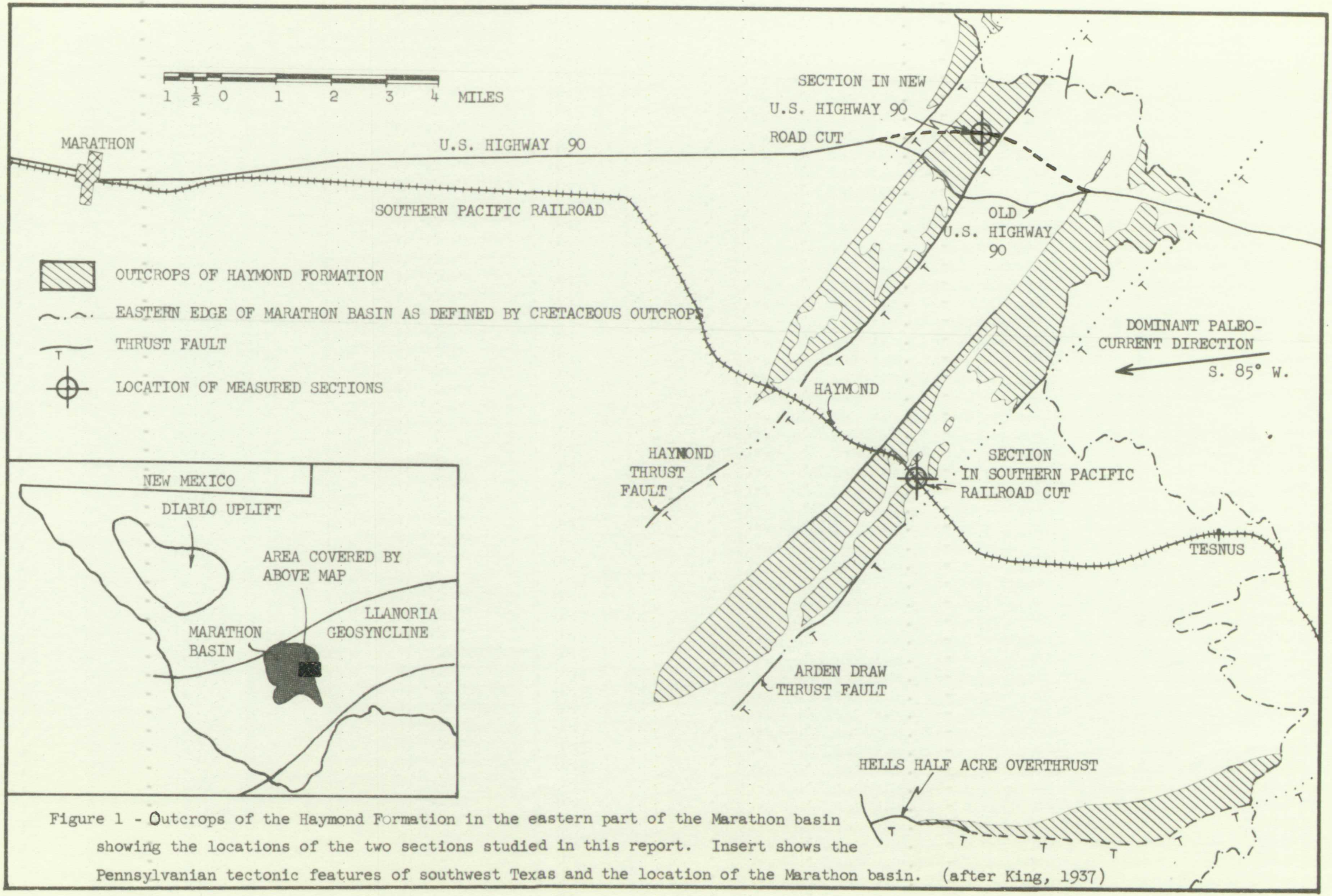

Figure 1 - Outcrops of the Haymond Formation in the eastern part of the Marathon basin showing the locations of the two sections studied in this report. Insert shows the Pennsylvanian tectonic features of southwest Texas and the location of the Marathon basin. (after King, 1937)

Purpose

The purpose of this investigation is to reconstruct the environment of deposition of the shale and siltstone of the Haymond Formation in order to understand the time relations of stratification in a marine slope environment.

Acknowledgments

The writer wishes to thank Dr. Roger Y. Anderson for suggesting the problem and for his guidance and many helpful suggestions throughout the study. Thanks are due to Dr. Sherman A. Wengerd and Dr. J. Paul Fitzsimmons of the thesis committee for their critical review of the report.

This study was supported in part by a research grant from the Earth Sciences Program of the National Science Foundation, Washington, D. C. (NSF-GP742). The X-radiographs were prepared by the Legant and Galloway X-ray Laboratories of Albuquerque. Financial assistance was generously given by the Roswell Geological Society.

The purpose [illegible]
environment [illegible]
[illegible]
of [illegible]

[illegible]

The writer wishes to express [illegible]
suggesting the [illegible]
suggestions [illegible]
Sherman [illegible]
committee for [illegible]

This study [illegible]
from the [illegible]
Foundation, [illegible]
were [illegible]
of Albuquerque [illegible]
by the [illegible]

STRATIGRAPHY AND STRUCTURE

The Haymond Formation was named by Baker (in Udden, Baker, and Böse, 1916, p. 46) from two exposures east and west of Haymond station on the Southern Pacific Railroad. Later, Baker (1917, p. 107) suggested that the Haymond Formation might actually be part of the Tesnus Formation that had been thrust across the Dimple Limestone. However, the validity of the Haymond Formation as a separate unit was demonstrated by King and King (1928, p. 113) with the discovery of boulders of Tesnus and Dimple in the boulder-bed member of the Haymond.

General characteristics

The Haymond Formation contains six members totaling over 3,000 feet in some places (King, 1937, p. 65). At the base of the formation, 300 feet of dark shale are followed by 1,000 feet of alternating siltstone and shale layers a fraction of an inch to over a foot thick (Figs. 2 and 3). These siltstone and shale layers are overlain by a thin (0-6 feet) layer of massive arkose followed by another sequence of alternating siltstone and shale 500 feet thick. This second siltstone-shale sequence is overlain by a 300 to 900 feet thick boulder-bed containing boulders of older rocks as long as 130 feet. At the top of the formation is a third sequence of alternating siltstone and shale 1,000 feet thick.

Figure 2 - Photographs of the two sections of the Haymond Formation studied in this report.

A. Cut in U. S. Highway 90, 15 miles east of Marathon. Measured section is indicated by solid lines; part of the section used for correlation is indicated by dashed lines.

B. Cut in Southern Pacific Railroad, 2 miles east of Haymond station. Section used for correlation is indicated by solid lines.

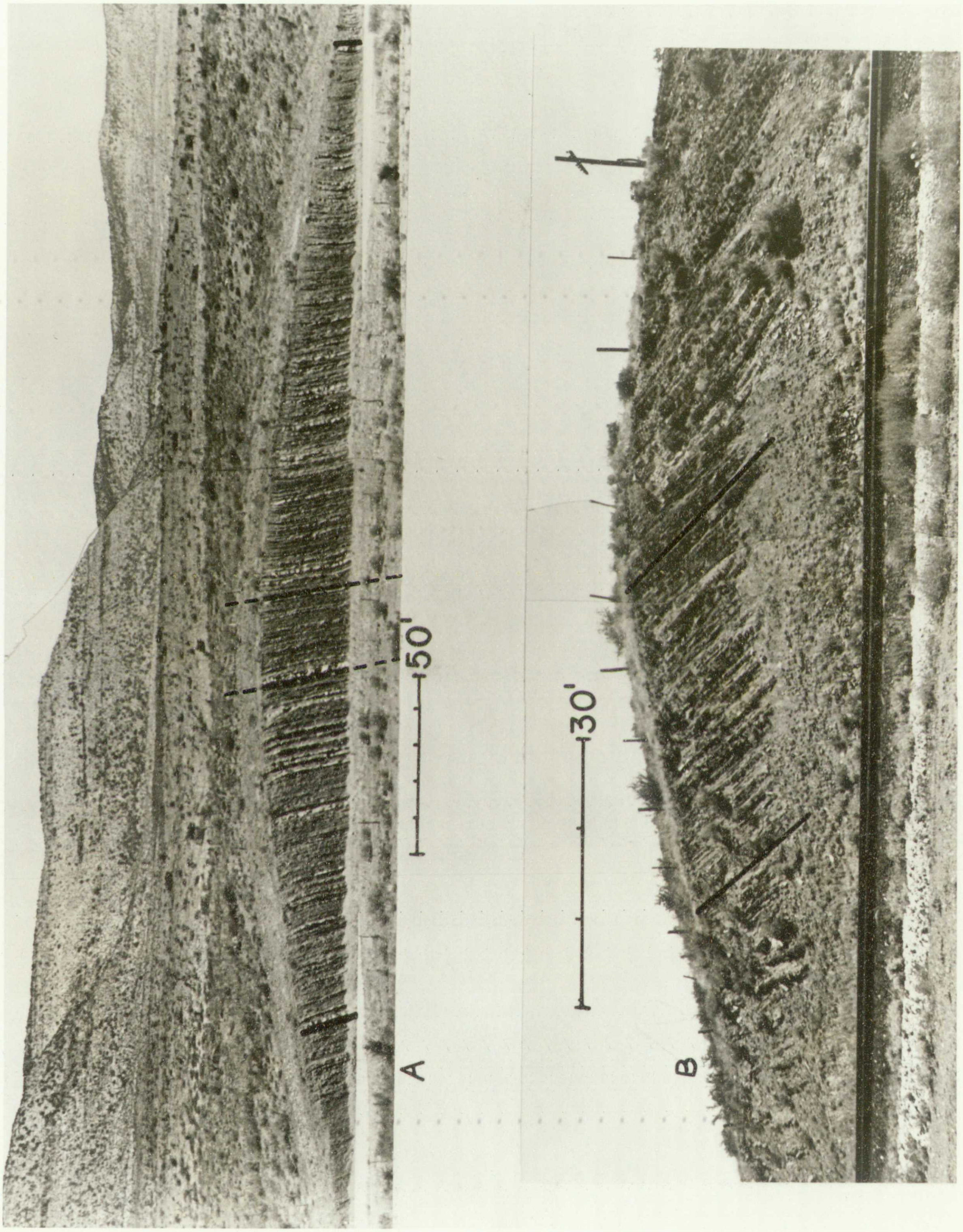
A
50'
B
30'

Figure 3 - Photographs of the sections of the Haymond Formation used for correlation.

A. Cut in U. S. Highway 90, 15 miles east of Marathon.

B. Cut in Southern Pacific Railroad, 2 miles east of Haymond station.

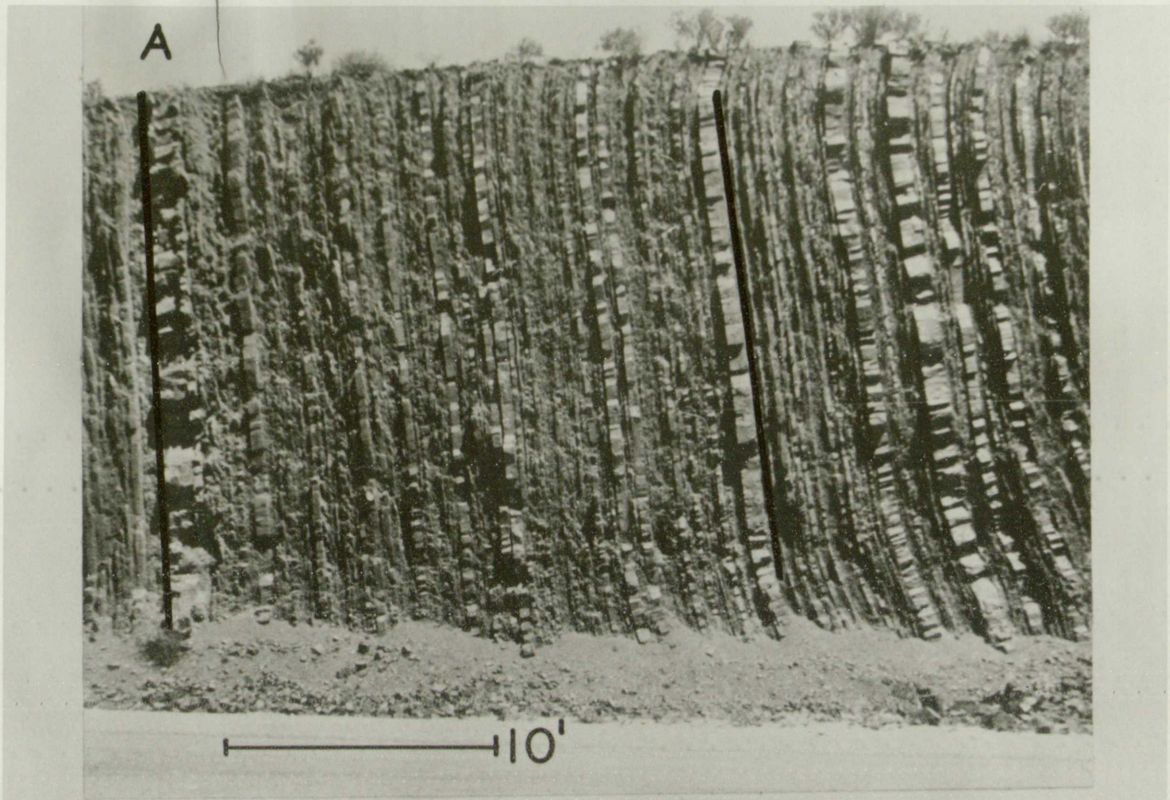
A
10'

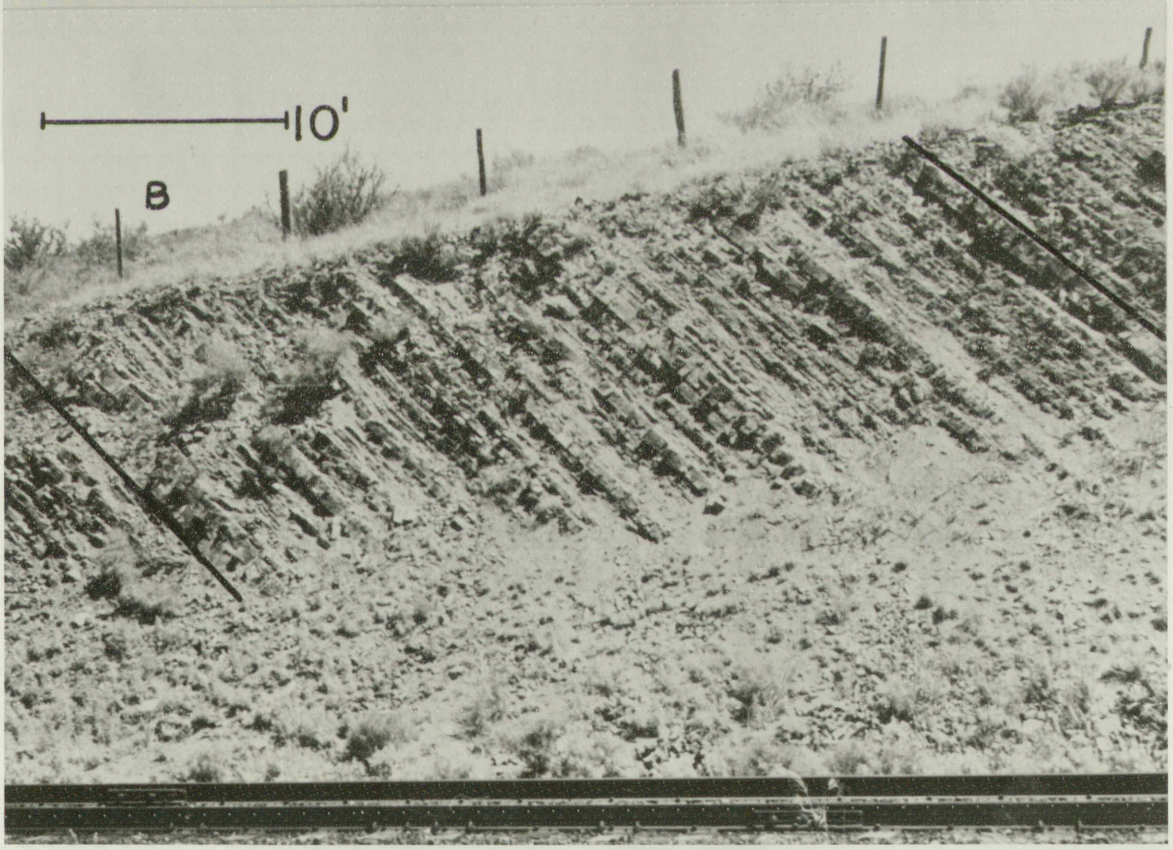
10'
B

Age and stratigraphic relations

The fossil content of the Haymond Formation consists mainly of abraded plant fragments a few of which were identified by David White and C. B. Read as being of Pottsville age (in King, 1937, p. 71). Fusulinids from the Haymond Formation collected by E. H. Sellards and C. L. Baker were identified as *Fusulina* by C. O. Dunbar (in King, 1937, p. 72). *Fusulina* ranges no higher than the Upper Desmoinesian Series (Strawn Series of central Texas). King concludes that the Haymond Formation is Lower Pennsylvanian as suggested by Girty (King, 1937, p. 72). Dunbar (1960, p. 224) places the Haymond Formation in the Atoka Series (Fig. 4).

The contact between the Haymond Formation and the underlying Dimple Limestone is vertically gradational for several hundred feet (King, 1937, p. 64; Sellards, Adkins, and Plummer, 1932). The Dimple Limestone represents a reduction in the supply of Tesnus material which was later resumed to produce the remarkably similar siltstone-shale alternations of the Haymond Formation. The contact between the siltstone and shale of the Haymond Formation and the overlying *Chaetetes*-bearing limestone of the Gaptank Formation is conformable and sharp (King, 1937, p. 72).

Based on subsurface data and lithologic similarity, the Haymond Formation has been correlated with the Smithwick and Big Spring Groups of central Texas and the Atoka Formation of southern Oklahoma (Plummer and Moore, 1921; Powers, 1928; Cheney, 1929; Moore, 1929; Miser and Sellards, 1931; Plummer, 1931; van der Gracht, 1931; King, 1937; Bokman, 1953; Hall, 1956; Cline, 1960; Dunbar, 1960; Miser and Hendricks, 1960).

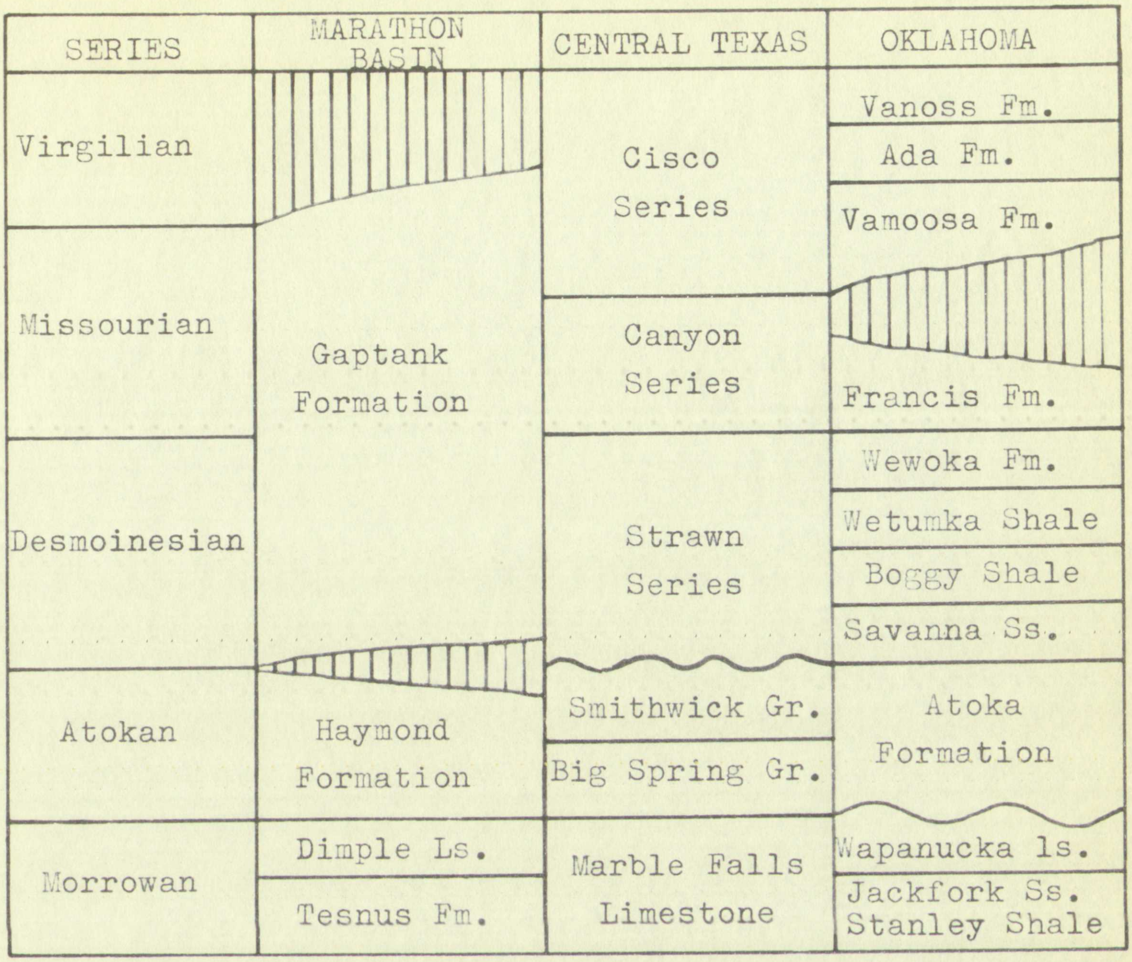

Figure 4 - Correlation of the Pennsylvanian System in southwest Texas, central Texas, and southern Oklahoma (after Dunbar, 1960, p. 224).

Structural history

Sedimentation was essentially continuous in the Marathon region during the Pennsylvanian. The sediments were deposited in the Llanoria geosyncline which was probably an extension of the Ouachita geosyncline of Oklahoma (Dunbar, 1960, p. 223; Sellards, Adkins, and Plummer, 1932, p. 129).

The beginning of the Pennsylvanian was marked by strong uplift of the hinterland (Llanoria) to the southeast exposing the granite, slate, and phyllite which provided the sediments

for the thick "flysch" sequence represented by the Tesnus and Haymond Formations (King, 1930 and 1937). The origin of the boulder-bed member of the Haymond Formation is not clear. Hall (1957 and 1959) suggests that the boulders are of tectonic origin. Other suggestions include glaciation (Baker, 1932; Carney, 1935), mudflow (King, 1937; Flawn, 1958), and subaqueous landslip (King, 1958). Gaptank time began with the deposition of the extensive Chaetetes-bearing limestone followed by "molasse" sedimentation (King, 1937, p. 88). By the end of Gaptank time, strong folding and overthrusting had produced a series of tightly folded mountain ranges of Paleozoic rocks (Baker and Bowman, 1917, p. 111). These ranges were eroded throughout the Triassic and Jurassic and the remnants covered by the Cretaceous Trinity and Fredericksburg Groups. During the Tertiary, probably post-Oligocene (King, 1937, p. 140), the Cretaceous sediments were uplifted to form the broad Marathon dome. The crest of the dome was eroded to expose the remnants of the tightly folded late Paleozoic mountain ranges in a topographic depression called the Marathon basin.

For the [illegible]

between [illegible]

coincide [illegible]

(1957 and 1958) [illegible]

within [illegible]

Germany (1965), [illegible]

[illegible]

of the [illegible]

[illegible]

PETROLOGY

General description

The two sections of the Haymond Formation which were studied are interbedded lentils of dense siltstone and clay shale. Many of the shales are separated by a thin, silty claystone intermediate in composition between the siltstone and shale. The siltstone occurs in layers 0.01 to 1.67 feet thick with a mean of 0.31 feet for the road-cut section and 0.43 feet for the railroad-cut section. The associated shale occurs in layers 0.01 to 1.26 feet thick. The siltstone-shale couplets range in thickness from 0.05 to 2.12 feet.

Petrography

Siltstone

The siltstone of the Haymond Formation has the composition of a subgraywacke although more than 70 percent of the grains are smaller than very fine sand (Fig. 5). Summaries of the chemical and mineralogical compositions are given in appendixes I and II and Figures 6 and 7. A photomicrograph of a typical siltstone is shown in Figure 8C. There is no significant change in siltstone composition throughout the section studied, with the possible exception of a general increase in the percent of organic nitrogen from the bottom of the section to the top (Fig. 9). The mineralogic composition of a typical siltstone is approximately: 70 percent quartz; 23 percent clay matrix; 3 percent plant fragments; 2 percent mica; 1 percent

RESULTS

General description

The two sections of the Bayard formation which were studied are interbedded lentils of dense siltstone and clay shale. Many of the shales are separated by a thin, silty claystone intermediate in composition between the siltstone and shale. The siltstone occurs in layers 0.[illegible] to 1.[illegible] feet thick with a mean of 0.[illegible] feet for the road-cut section and 0.45 feet for the railroad-cut section. The associated shale occurs in layers 0.02 to 1.76 feet thick. The siltstone-shale couplets range in thickness from 0.0[illegible] to 2.12 feet.

Petrography

Siltstone

The siltstone of the Bayard formation has the composition of a subgraywacke although more than 50 percent of the grains are smaller than very fine sand (Fig. 5). Summaries of the chemical and mineralogical compositions are given in Appendixes I and II and Figures 6 and 7. A photomicrograph of a typical siltstone is shown in Figure 8. There is no significant change in siltstone composition throughout the section with the possible exception of a general decrease in the percent of organic nitrogen from the bottom of the section to the top (Fig. 9). The mineralogic composition of the siltstone is approximately 70 percent quartz; [illegible] clay matrix; 5 percent plant fragments; [illegible] albite; 1 percent garnet. These constituents suggest igneous and possibly metamorphic terranes. King (1937, p. 70) concluded that the constituents of the Haymond siltstone were derived from granitic and metamorphic rocks with the granitic fragments predominating. McBride (1962b) concluded that the chief source area of the Haymond sediments was composed largely of plutonic rocks.

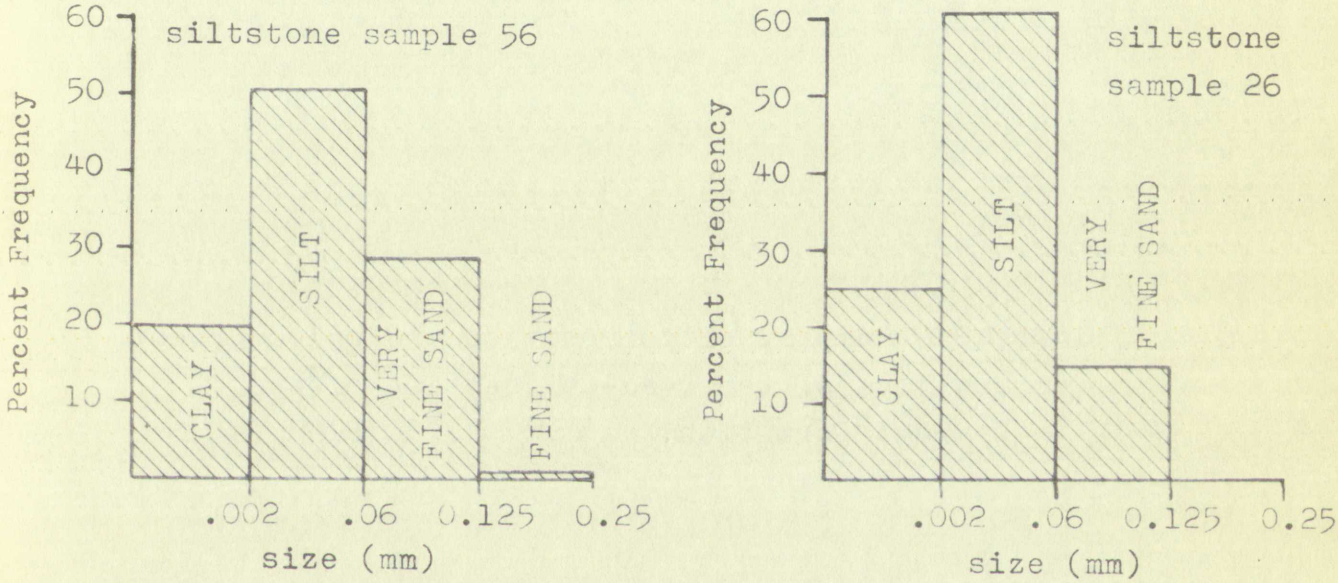

Figure 5 - Grain size determinations of two siltstone samples of the Haymond Formation. Percent clay was estimated; percent silt and sand were determined by counting about 500 grains in thinsection.

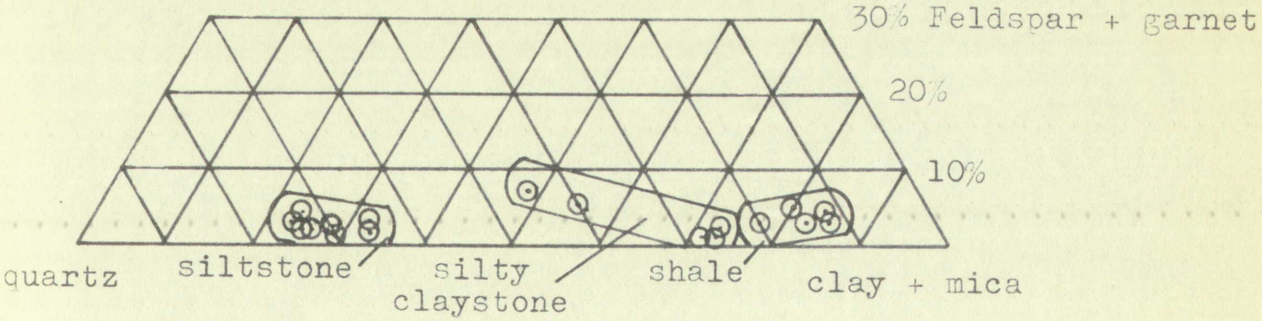

Figure 6 - Composition of siltstone, silty claystone, and shale of the Haymond Formation.

Figure 7 - Summary of composition and paleocurrent analyses of the road-cut section of the Haymond Formation.

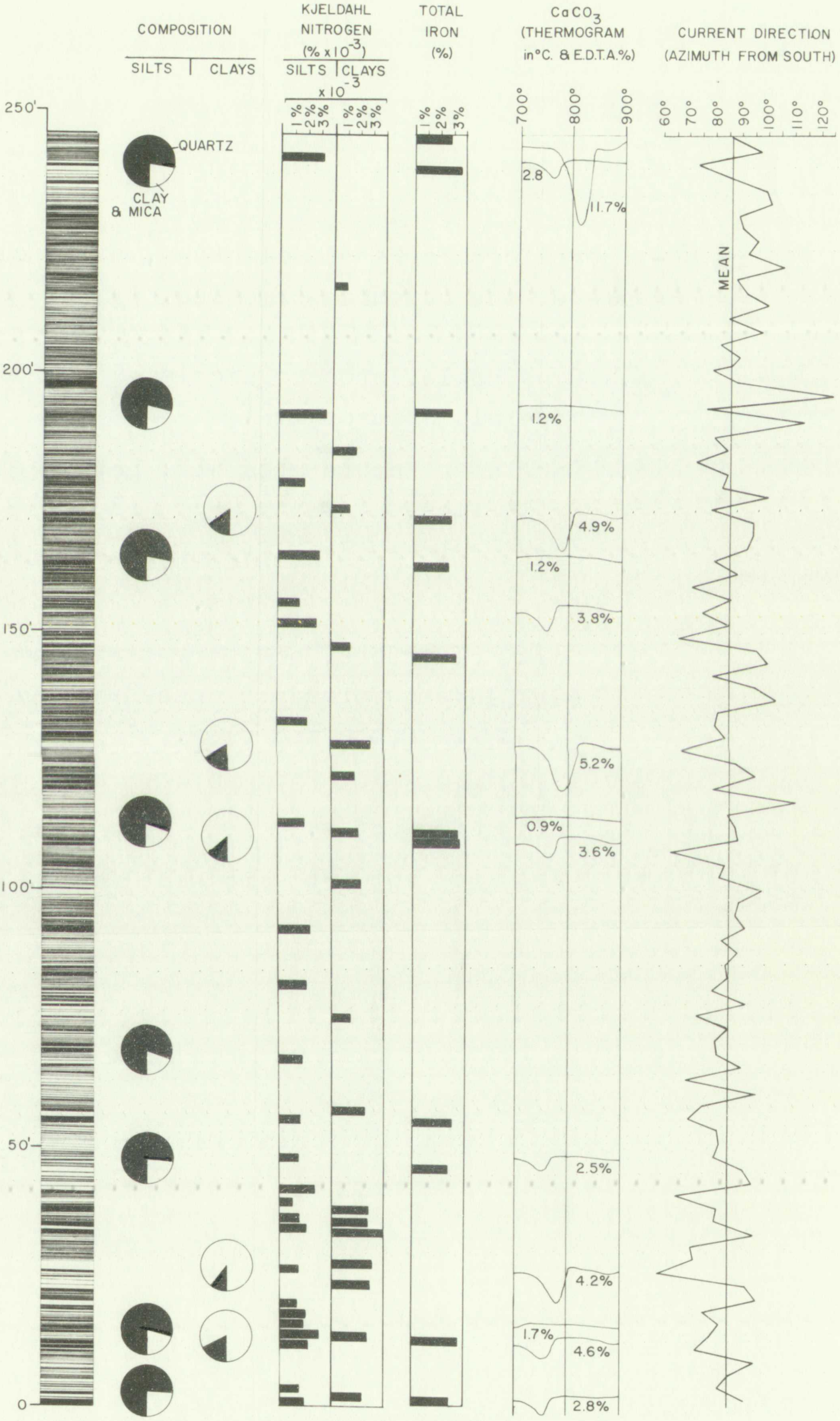
COMPOSITION
SILTS | CLAYS
KJELDAHL NITROGEN (% x 10^-3)
SILTS | CLAYS
x 10^-3
1% 2% 3%
TOTAL IRON (%)
CaCO3 (THERMOGRAM in °C. & E.D.T.A.%)
700° 800° 900°
CURRENT DIRECTION (AZIMUTH FROM SOUTH)
60° 70° 80° 90° 100° 110° 120°
250'
200'
150'
100'
50'
0
QUARTZ
CLAY & MICA
MEAN
2.8
11.7%
1.2%
4.9%
1.2%
3.8%
5.2%
0.9%
3.6%
2.5%
4.2%
1.7%
4.6%
2.8%

Figure 8 - Photomicrographs of siltstone, silty claystone, and shale of the Haymond Formation.

A. Clay shale, crossed nicols, x300; linear mineral is muscovite.

B. Same as A but rotated 45°; note aggregate extinction.

C. Siltstone, crossed nicols, x300; mainly quartz in a clay matrix.

D. Silty claystone, ordinary light, x46; note dark layers formed by concentration of plant fragments and clay.

E. Silty claystone, ordinary light, x150; enlargement of D.

F. Same as E but with crossed nicols.

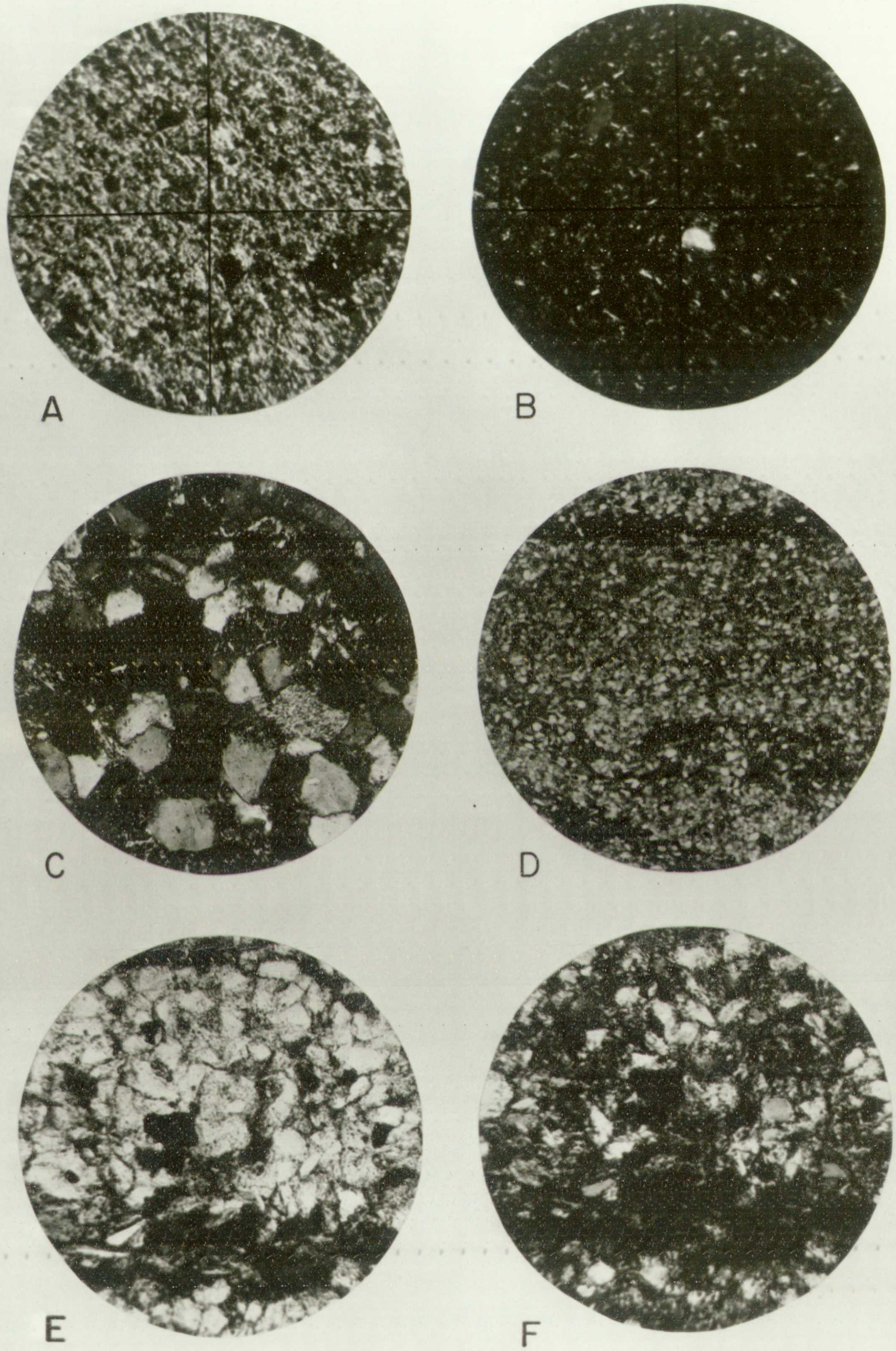
A
B
C
D
E
F

Quartz. - - Quartz occurs as angular, silt grains with numerous inclusions and few overgrowths. Where the grains are elongate, they are subparallel to the parallel fabric of the mica and clay minerals.

Plagioclase feldspar. - - Plagioclase occurs as angular, silt grains easily distinguished from quartz by the multiple albite extinction bands and lower index of refraction. The low extinction angles (17 degrees to 18 degrees) and low index of refraction place the plagioclase at the albite end of the albite-anorthite series (Kerr, 1959, p. 258).

Garnet. - - Garnet occurs as angular, pale yellow and pale pink silt grains. The grains are identified by their isotropism and high relief.

Muscovite. - - Muscovite occurs as colorless shreds parallel to stratification. Under crossed nicols, these shreds have a brilliant, high-order green or blue interference color and parallel extinction.

Biotite. - - In some samples, shreds of biotite were distinguished from muscovite shreds by their darker color and strong pleochroism.

Clay. - - A clay matrix constitutes as much as 26 percent of the siltstone. Positive identification of clay minerals other than small amounts of sericite was not possible in thin-section

but differential thermal analyses of 20 siltstone and shale samples indicated a probable mixture of chlorite and illite (Grim, 1953, p. 198).

Because thin-sections were cut normal to stratification, plates of clay and mica present an edge view parallel to the c-axis with consequent parallel extinction. This parallel extinction of individual minerals produces an aggregate extinction of the clay matrix as illustrated in Figures 8A and 8B.

Plant fragments. - - Six siltstone and shale samples were treated with hydrochloric, hydrofluoric, and nitric acids. The residue consisted almost entirely of black plant fragments. The concentration of plant fragments with clay and mica into layers parallel to stratification produces the laminated appearance of the shale and siltstone (Figs. 8D, 8E, and 8F). The plant fragments are also concentrated along cross-stratification planes in the siltstone.

Silty claystone

Intermediate in composition between the siltstone and shale are a group of laminae, generally less than 0.05 feet thick, classified as silty claystone. The quartz content of the silty claystone varies from 25 percent to 45 percent and the clay content from 25 percent to 60 percent (Appendix I; Fig. 6). Although the composition of the silty claystone is considerably more variable than that of either the siltstone or shale, it is closer to that of the shale. However, because the quartz content of the silty claystone is higher than that of the shale, the but differential thermal analyses of 20 [illegible] samples indicated a probable presence of chlorite and illite (Grim, 1953, p. 192).

Because thin-sections were cut normal to stratification, plates of clay and mica present a side view parallel to the c-axis with consequent parallel extinction. This parallel extinction of individual [illegible] aggregate extinction of the clay matrix as illustrated in [illegible]

Plant fragments. - - Six siltstone and shale samples were treated with hydrochloric, hydrofluoric, and nitric acids. The residue consisted almost entirely of [illegible] plant fragments. The concentration of plant fragments with clay and mica into layers parallel to stratification produces the laminated appearance of the shale and siltstone (Figs. 20, 21, and 27). The plant fragments are also concentrated along cross-stratification planes in the siltstone.

Silty claystone

Intermediate in composition between the siltstone and shale are a group of lutites, generally less than 0.05 foot thick, classified as silty claystone. The quartz content of the silty claystone varies from 25 percent to 45 percent and the clay content from 35 percent to 60 percent (Appendix [illegible]). Although the composition of the silty claystone is [illegible] more variable than that of either the siltstone or shale, it is closer to that of the shale. However, because the [illegible] of the silty claystone is higher [illegible] weathering characteristics closely resemble those of the siltstone. Consequently, the silty claystone was counted as siltstone in statistical analyses. The feasibility of this grouping will be demonstrated later in this report.

Shale

The mineralogical composition of a typical shale in the Haymond Formation is approximately: 73 percent clay minerals; 15 percent quartz; 5 percent mica; 4 percent plant fragments; 2 percent garnet; <1 percent albite. Summaries of the chemical and mineralogical compositions of the shale are given in Appendixes I and II and Figures 6 and 7. The descriptions of the specific minerals given for the siltstone also apply to the minerals of the shale. There is no significant change in the composition of the shale throughout the section with the possible exception of a general decrease in organic nitrogen content from bottom to top in the section (as opposed to an increase in organic nitrogen in the siltstone) (Fig. 9). Photomicrographs of a typical shale are shown in Figures 8A and 8B.

At the surface, the shale is fissile and erodes into small, lenticular chips. On a fresh surface, however, the fissility is obscure and the shale breaks into rounded discs several inches in diameter which further spall into thin concentric sheets. The tendency of the clays to split into thin sheets is the result of parallel alignment of the clay minerals and mica. The curving of the sheets is probably a result of rotation of the clay and mica during intense folding.

Chemical Analyses

Calcium and Magnesium Carbonate

The amount of calcium and magnesium carbonate in 15 samples was determined by titrating with disodium dihydrogen ethylenediamine tetracetate (Na_2EDTA or EDTA) (Bisque, 1961). As calcium from gypsum and illite may go into solution during treatment with hydrochloric acid, there is a certain amount of error to be expected by using this method to determine calcium and magnesium carbonate. Sulfate tests were run on two samples with results of 1.4 percent and 0.24 percent; thus the amount of gypsum present is negligible for the purpose of this study. Also, the amount of calcium derived from illite is probably negligible so that the results are probably correct to within 5 percent of the amount present. Neither calcium nor magnesium content show a significant trend throughout the section. The amount of calcium carbonate ranges from 0.9 percent to 11.7 percent. The amount of magnesium carbonate ranges from a trace to 1.0 percent. EDTA percentages of calcium and magnesium carbonate are listed in Appendix II. EDTA percentages of calcium carbonate are also given in Figure 7 with the corresponding thermogram peaks for calcium carbonate.

Iron

The amount of iron in 15 samples was determined by colorimetry. The results are expressed as ferric iron as all ferrous iron is oxidized during the procedure (Appendix II;

Fig. 7). The range [illegible] percent and [illegible] to [illegible] [illegible]. The percent of [illegible] grade in each of the 15 samples can be obtained [illegible] multiplying the total [illegible] percent by 1.43.

Organic Nitrogen

The amount of organic nitrogen in 14 samples was determined by the Kjeldahl method; the organic nitrogen was converted to ammonia by Kjeldahl digestion and the ammonia [illegible] determined by colorimetry (Appendix II, Figs. 7 and 8). The organic nitrogen content ranges from 0.010 percent to 0.[illegible] percent. The percent of organic material in each sample may be approximated by multiplying the organic nitrogen percent by 17 (Hillsman and Emery, 1951, p. 205).

In general, the percent of organic nitrogen in the silty and silty [illegible] samples increases from the bottom of the section to the top whereas the percent of organic nitrogen in the siltstone samples increases (Fig. 14). This is a further indication of the depositional similarity of the shale and silty claystone. The greatest difference between the percent of organic nitrogen in the siltstone and shale samples occurs in the part of the section containing the [illegible] lowest [illegible] siltstone and shale layers (compare Figure 7 with Figures 14, 15, 16, and 17).

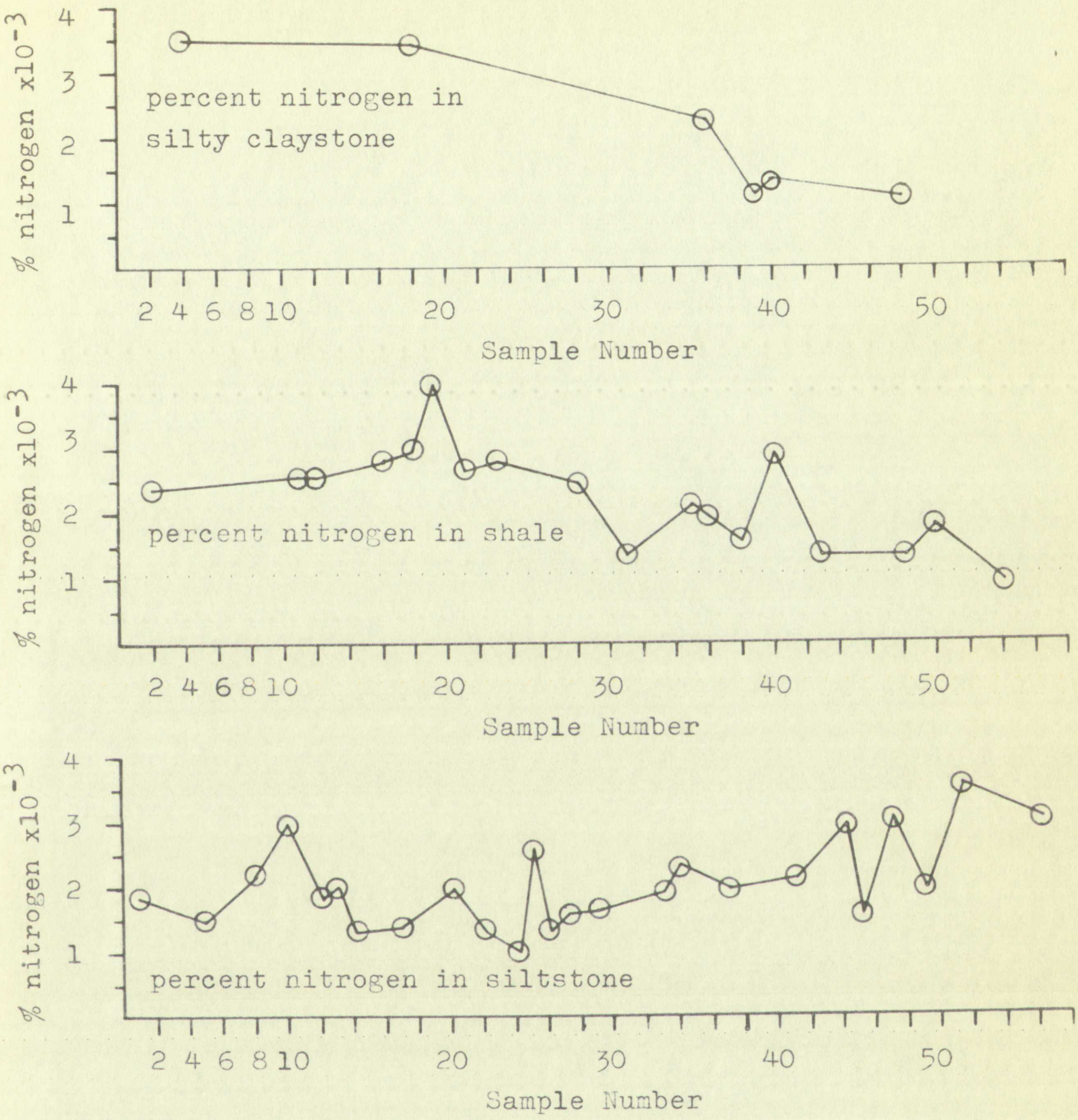

Figure 9 - Variation of organic (Kjeldahl) nitrogen in the silty claystone, shale, and siltstone samples of the Haymond Formation. (See Figure 18 for location of samples.)

Sedimentary structures

Stratification

The alternations of siltstone and shale, repeated thousands of times throughout several thousand feet of section, are the most obvious sedimentary structures in the Haymond Formation (Figs. 2 and 3). At a distance, the boundaries between the siltstone and shale appear sharp. On closer inspection, it is apparent that the contact between a siltstone and the underlying shale is always sharp whereas the same siltstone grades more or less rapidly into the overlying shale (Fig. 10). The gradation is one of composition with an increase

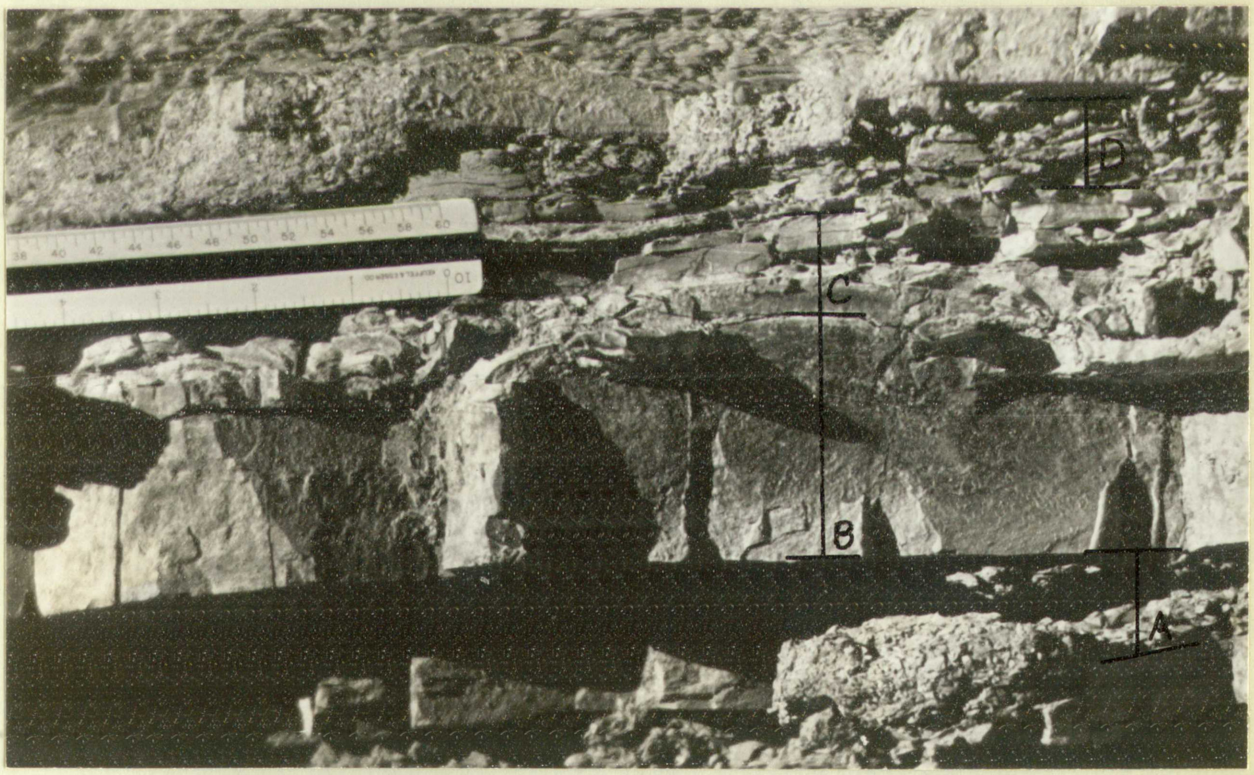

Figure 10 - Gradational contact (C) between a siltstone (B) and the overlying shale (D); note the sharp contact between the siltstone (B) and the underlying shale (A).

in clay and a decrease in quartz between the siltstone and shale. As most of the quartz is silt, this gradation is also one of size. As a consequence, the difference in bedding of the siltstone and shale is the result of differences in composition; however, the differences in composition are the result of a decrease in silt, thereby increasing the relative proportions of clay.

A variation in grain size can be the result of one or a combination of two factors: 1. the amount and type of sediment available and 2. the efficacy of the scattering agent. Because of the frequency with which the siltstone layers recur, it does not seem probable that the cyclic alternations are a function of availability although the availability may effect long term cyclic or non-cyclic variations (Fig. 14). It is probable, therefore, that the deposition of a silt layer is initiated by a current capable of transporting silt and waning of the current permitting settling of clay.

Internal structures

Recognition of most internal sedimentary structures is based on differences in color, composition, or texture which are the result of physical processes operative at the time of deposition. The siltstone and shale layers of the Haymond Formation have sedimentary structures so subtile that they are barely visible even on polished surfaces. To accentuate these structures, four techniques were applied to slabs of siltstone cut normal to stratification: infra-red photography, dye staining, X-radiography, and etching with hydrofluoric acid.

in clay [illegible]
shale. [illegible]
also due [illegible]
of the extreme [illegible]
composition [illegible]
result of [illegible]
proportions of clay.

A variation in [illegible]
combination of [illegible]
available and [illegible]
of the [illegible]
not seem [illegible]
of [illegible]
cyclic or non-cyclic [illegible]
therefore, [illegible]
a current [illegible]
period [illegible]
[illegible]
internal [illegible]

Recognition [illegible]
based on [illegible]
are the result [illegible]
of deposition. [illegible]
Formation have [illegible]
[illegible]
structures, [illegible]
[illegible]

Only the last two techniques succeeded in accentuating the internal sedimentary structures (Figs. 11 and 12). Exposing a slab to infra-red sensitive film using only an infra-red light source produced results no better than those obtained using white light and panchromatic film. Compositional differences apparently were not great enough to permit differential absorption of infra-red light. These small compositional differences in addition to very low permeability prevented the use of dye staining techniques (Hamblin, 1962a; Pantin, 1960).

Recently, application of X-radiography to the study of internal sedimentary structures has been successful in both consolidated (Hamblin, 1962b) and unconsolidated sediments (Calvert and Veevers, 1962). The technique is based on the concept that there should be vertical as well as lateral variations in every sedimentary rock. These variations should produce corresponding variations in density even though there may be no corresponding variation in color or texture. The transmission of X-rays through a slab of a sedimentary rock records density variations by differential absorption of radiation. Slabs of several siltstone samples approximately 3 mm thick were placed directly on X-ray film and exposed at a distance of about one meter at 50 kilovolts and 125 milliamperes for one second using a General Electric medical X-ray unit. Positive prints of radiographs are shown in Figures 11C, 11D, 12B, and 12E. In most slabs, remarkably clear outlines of internal sedimentary structures were obtained even though the structures were invisible or only faintly visible on polished slabs (Figs. 11A, 11B, 12A, and 12D). This technique was particularly useful in accentuating cross-laminations.

Figure 11 - Sedimentary structures in two treated siltstone slabs from the Haymond Formation.

A. Polished siltstone slab.

B. Polished siltstone slab.

C. X-radiograph of siltstone slab in A.

D. X-radiograph of siltstone slab in B.

E. Hydrofluoric acid etch of siltstone slab in A.

F. Hydrofluoric acid etch of siltstone slab in B.

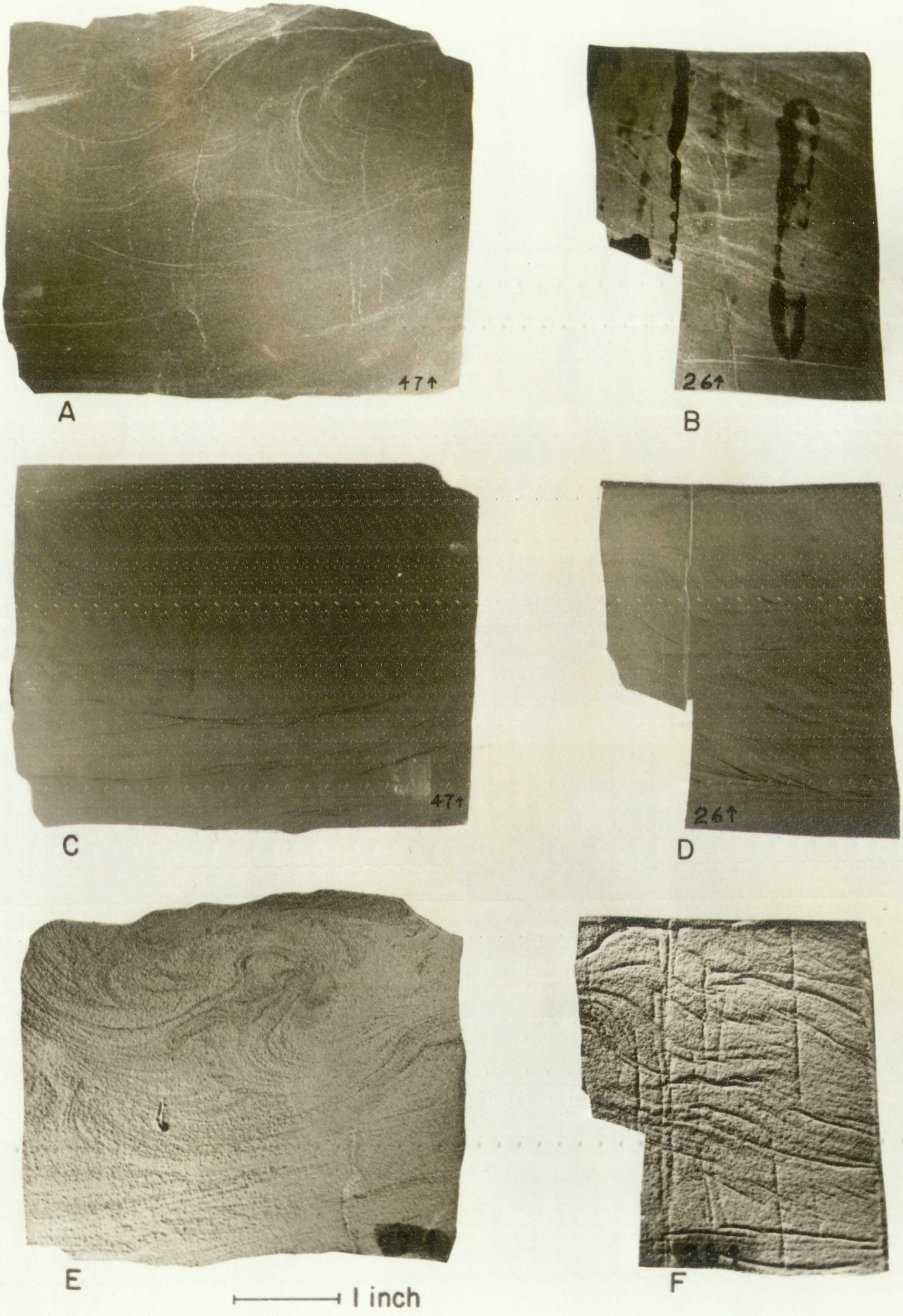
47↑
A
26↑
B
47↑
C
26↑
D
E
F
1 inch

Figure 12 - Sedimentary structures in two treated siltstone slabs from the Haymond Formation.

A. Polished siltstone slab.

B. X-radiograph of siltstone slab in A.

C. Hydrofluoric acid etch of siltstone slab in A.

D. Polished siltstone slab.

E. X-radiograph of siltstone slab in D.

F. Hydrofluoric acid etch of siltstone slab in D.

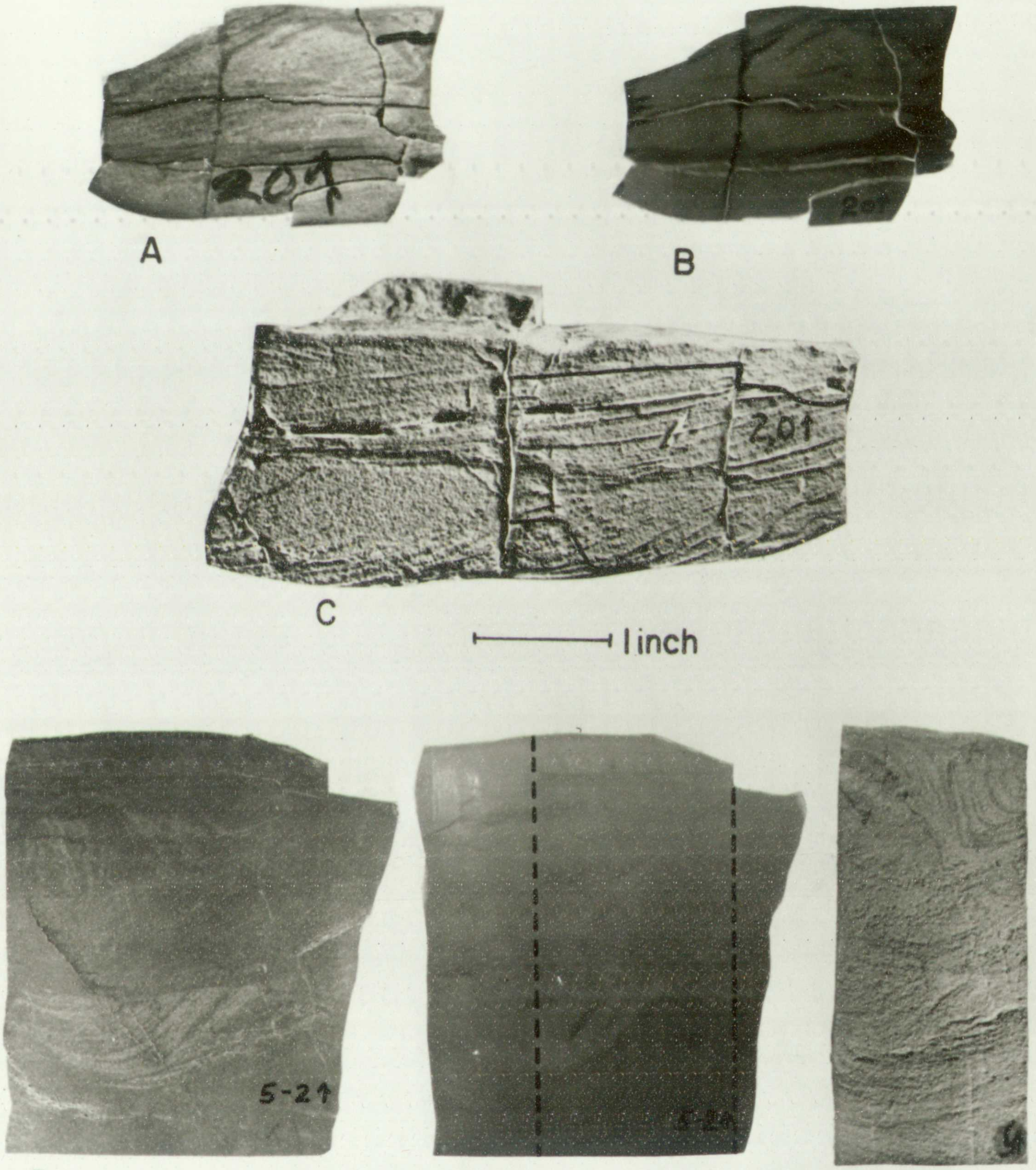
A
B
C
1 inch
5-2↑
D
E
F

In most slabs, internal structures, particularly convolute folds, were emphasized by etching with hydrofluoric acid. This was done be immersing a slab or a flat surface of siltstone in concentrated hydrofluoric acid for several hours. After the etched surfaces had been washed and dried, they were photographed using a single low-angle light source. Photographs of etched siltstones are shown in Figures 11E, 11F, 12C, and 12F.

<u>Horizontal laminations</u>. - - In addition to the gross stratification or lamination, some of the individual siltstone or shale layers are also laminated on a semi-microscopic scale. These micro-laminations are the result of the concentration of plant fragments, clay, and mica into dark bands parallel to stratification (Figs. 8D, 8F, and 8F). Micro-laminations in the shale are almost always horizontal whereas those in the siltstone are more often contorted into convolute folds (Figs. 11E and 11F). The micro-laminations are not sedimentary units but represent "transitory 'phases' or minor chance fluctuations in the velocity of the depositing current" (Pettijohn, 1957, p. 163).

<u>Cross-laminations</u>. - - Small-scale tabular cross-laminations are present in many of the siltstone layers. Although cross-laminations are usually confined to the lower part of the layer (Figs. 11C to 11F), some layers are cross-laminated throughout their entire thickness (Fig. 12C). The cross-laminations represent deposition by unidirectional laminar current flow. Although most of the cross-laminations are tabular, several scour-and-fill cross-laminations were also noted (Figs. 12D to 12F).

Convolute-laminations. - - Convolute-laminations, as applied here, refer to contorted or wavy laminae observed in the upper part of many siltstone layers. The contortions range from gentle crenulations to highly contorted folds which die out downward into undisturbed cross-laminations in the lower part of the layer (Figs. 11E and 11F). Folded patterns generally consist of a series of steeply dipping, usually overturned anticlines separated by broad shallow synclines. The convolute-laminations were probably deposited as horizontal or cross-laminations which were later contorted. Convolute-laminations have been the subject of frequent discussions in the literature (Kindle, 1917; Bain, 1931; Rettger, 1935; Jones, 1937; Baldry, 1938; Lamont, 1938; Beets, 1946; Cope, 1946; Kuenen, 1949; Rich, 1950 and 1951; Kuenen, 1953; Greensmith, 1956; Stewart, 1956; Ten Haaf, 1956; Sullwold, 1959; Holland, 1960; Prentice, 1960; Sanders, 1960; Williams, 1960; Dott and Howard, 1962; McBride, 1962a). Most agree that the contortions are the result of plastic deformation in response to gravity. The uniform lateral thickness of the siltstone layers, even though the laminae within the layer are highly contorted, precludes mass downslope translation or slump. Saturated with water, the silt layer was essentially a viscous fluid with a tendency to flow downslope under the influence of gravity. Adhesion and cohesion, resulting from a combination of electrolytic attractions, van der Waals forces, and surface adsorption of water (Dott and Howard, 1962, p. 115), prevented the mass from actually flowing. Instead, a certain amount of internal adjustment took place producing varying degrees of distortion. Most of this adjustment took

place before deposition of the overlying clay so that the upper part of the silt layer was less confined than the lower part of the layer. As a result, the upper part of the layer was more distorted, the contortions dying out downward into the lower part of the layer which remained in place due to increased internal cohesion and adhesion and friction between the silt layer and the underlying clay layer. This explanation seems to fit best the origin of the convolute siltstone laminae in the Haymond Formation.

Graded bedding. - - Graded bedding is present in the siltstone layers of the Haymond Formation only in a subtle form. The most noticeable grading is in the upper part of the siltstone which grades into the overlying shale by a decrease in silt. Bailey (1930) concluded that cross bedding and graded bedding represent deposition under two different conditions. Cross bedding is a document of current deposition whereas graded bedding is a document of gravity settling in still water. Recent studies by Kuenen (Kuenen and Migliorini, 1950; Kuenen and Menard, 1952; Kuenen, 1953), have led to the conclusion that, in most cases, graded bedding implies turbidity currents. Unfortunately, recent workers have frequently reversed this implication, i.e. turbidity currents imply graded bedding. This latter implication is dependent upon the position of the particular section being studied with respect to the slope and the bottom of the basin of deposition. At the bottom of the basin, the turbidity current encounters a decrease in slope and the suspended load is "dumped". Turbulence continues, place before deposition of the overlying clay so that the upper part of the silt layer was less confined than the lower part of the layer. As a result, the upper part of the layer was more distorted, the contortions dying out downward into the lower part of the layer which remained in place due to increased internal cohesion and adhesion and friction between the silt layer and the underlying clay layer. This explanation seems to fit best the origin of the convolute siltstone laminae in the Beyond Formation.

Graded bedding. - Graded bedding is present in the siltstone layers of the Beyond Formation only in a subtle form. The most noticeable grading is in the upper part of the siltstone which grades into the overlying shale by a decrease in silt. Bailey (1930) concluded that cross bedding and graded bedding represent deposition under two different conditions. Cross bedding is a document of current deposition whereas graded bedding is a document of gravity settling in still water. Recent studies by Kuenen (Kuenen and Migliorini, 1950; Kuenen and Menard, 1952; Kuenen, 1953), have led to the conclusion that, in most cases, graded bedding implies turbidity currents. Unfortunately, recent workers have frequently reversed this implication, i.e. turbidity currents imply graded bedding. This latter implication is dependent upon the position of the particular section being studied with respect to the slope and the bottom of the basin of deposition. At the bottom of the basin, the turbidity current encounters a decrease in slope and the suspended load is "dumped". Turbulence continues, however, with little lateral movement until downslope movement has ceased. Because currents are absent, differential settling in response to gravity produces a graded sequence. On the slope, this "dumping" does not take place. Instead, the velocity of the turbidity current gradually decreases until laminar flow permits settling of material which is then deposited in cross-laminations.

Sole markings

Many of the lower bedding planes of siltstone layers of the Haymond Formation contain subparallel flute casts (Crowell, 1955, p. 1359) and groove casts (Shrock, 1948, p. 163). The flute and groove marks or depressions were formed on the upper surface of a clay layer by a silt-laden current. As the silt was deposited, it filled in the depressions in the underlying clay, forming a cast which was preserved on the lower bedding plane or sole of the silt layer. Features which seem to fit the description of flute casts as suggested by Crowell (1955, p. 1359) have been called lobate rill marks (Clarke, 1918; Shrock, 1948), flow markings (Rich, 1950 and 1951; Kuenen and Carozzi, 1953; Kuenen and Sanders, 1956), flow-roll markings (Rich, 1950), Strömungs-Marken (Rücklin, 1938), Gefliess-Marken (Richter, 1935), and spatulate casts (Pettijohn, 1957). For additional information on the origin and classification of these and similar markings, see the works of Rich and Wilson (1950), Prentice (1956 and 1960), Kelling and Walton (1957), Kuenen (1957), Kuenen and Prentice (1957), Crowell (1958), Glaessner (1958), Hsu (1958 and 1959), Kuenen and Ten Haaf (1958), Sullwold (1959), Holland (1960), Johnson (1962), and McBride (1962b).

however, with little [illegible] has ceased. [illegible] in response to [illegible] this "dumping" [illegible] the turbidity [illegible] permits settling [illegible] laminations.

Sole markings

Many of the lower [illegible] the Wayvond Formation contain [illegible] 1956, p. 1559) and groove [illegible] Flute and groove [illegible] surface of a clay layer [illegible] was deposited, it filled [illegible] clay, forming a [illegible] plane or sole of the [illegible] the description [illegible] p. 1559) have been called [illegible] Shrock, 1948), flow markings [illegible] Carozzi, 1955; Kuenen and Sanders [illegible] (Rich, 1950), [illegible] Marken (Hinton, [illegible] For additional information [illegible] these and similar [illegible] (1950), Prentice [illegible] Kuenen (1957), [illegible] Sullwold (1959), [illegible]

The orientations of 357 flute and groove casts were measured on the lower bedding planes of 107 siltstone layers throughout the road-cut section of the Haymond Formation. Strike and dip of individual layers were recorded along with the rake of each flute or groove cast. Using a stereonet, the layers were rotated to horizontal and the true orientations of the casts determined (Billings, 1954, p.485). Because the casts are linear features, their orientations may have one of two directions. The correct direction was determined by noting the bulbose (upcurrent) end of the flute cast.

Corrected directions of all flute and groove casts range from 55 degrees to 128 degrees (azimuth from the south) with a mean of 85.71 degrees and a standard deviation of 13.5 degrees. The directions were divided into 15 class intervals of 5 degrees each and the frequency distributions plotted as a histogram and as a rose diagram (Fig. 13). In the rose diagram, the length of each arrow, plotted on the midpoint of the class interval, is proportional to the number of measurements within that class interval. In addition, the mean direction was determined for each siltstone from which measurements were obtained and plotted in Figure 7. A summary tabulation of these measurements is given in Appendix III.

Figure 13 indicates an east to west paleocurrent direction with relatively little variation. These results confirm McBride's report (1962a) of an eastern source area with turbidity current flow ranging from transverse to parallel to the basin axis. Each point on the current variation curve (Fig. 7) represents the dominant current direction during deposition of

that particular silt layer. Although the variations in direction appear random, there is a noticeable trend from a southwesterly to a northwesterly direction perhaps indicating a minor change in the configuration of the edge of the basin (Fig. 7).

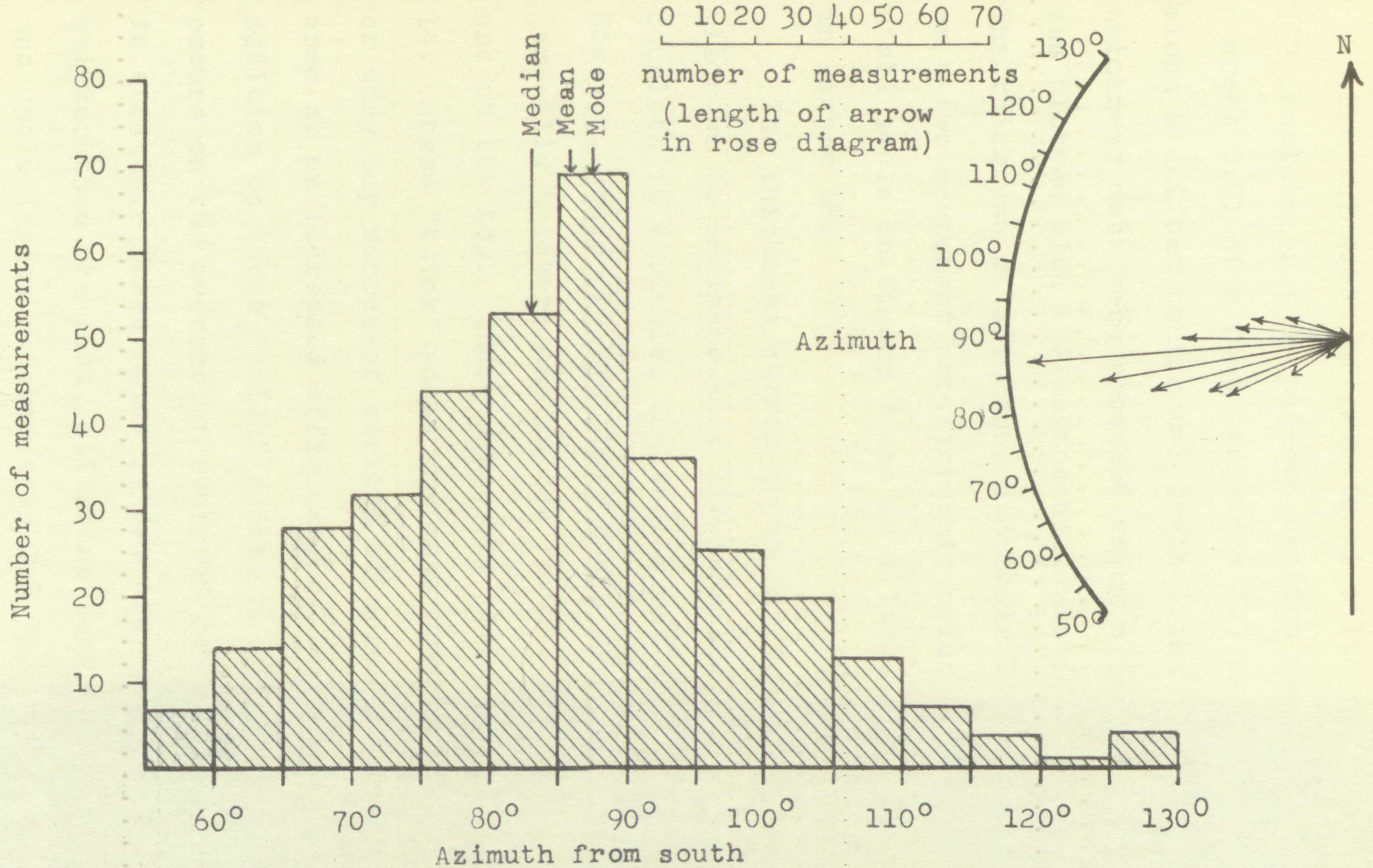

Figure 13- Variations in direction of flute and groove casts in the Haymond Formation.

STATISTICAL ANALYSES

The thickness of individual siltstone and shale layers of 767 couplets in the road-cut section were measured to the nearest 0.01 of a foot (Appendix IV) and plotted separately along a uniform horizontal scale (Figs. 16 and 17). Couplet thickness data were smoothed using a 31-unit moving average and plotted with the unsmoothed data in Figures 14 and 15. The thickness of siltstone and shale layers were then plotted as a two component stratigraphic column and presented on a small scale in Figure 7 and on a larger scale in 5 segments in Figure 18.

The thickness curves shown in Figures 14, 15, 16, and 17 all seem to indicate that although the thickness of individual couplets is variable, the variations are essentially random. However, there are two broad zones where the couplets are generally thicker; one in the lower quarter of the section and one at the top. These zones are the prominant highs in Figure 14. These "thick" zones may have some climatic significance, or they may represent periods of more active uplift of the source area or an increased efficiency of the scattering agent. In addition to these "thick" zones, an individual thick layer occurs on the average of every 40 couplets although the variation is erratic. These thick layers are represented by couplets thicker than one foot, siltstone layers thicker than 0.6 foot, and shale layers thicker than 0.5 foot (Figs. 15, 16, and 17).

The frequency distributions of siltstone and shale thickness for both the road-cut and railroad-cut sections are skewed to the

Dean- Slope- deposits- haymond- formation

Figure 14 - 31-unit moving average of silt-clay couplet thickness in the Haymond Formation

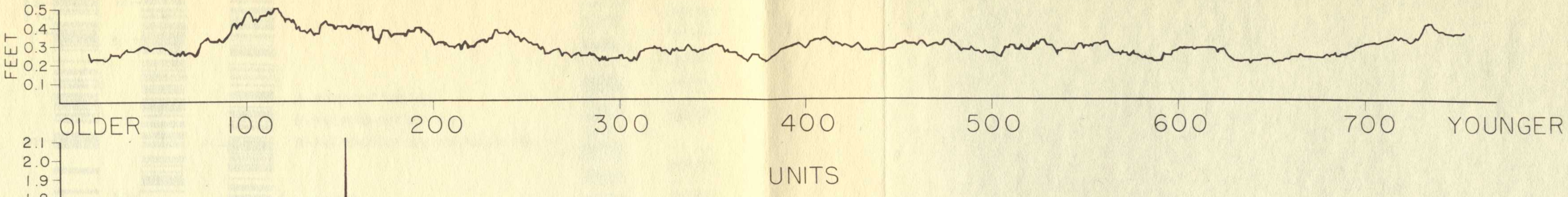

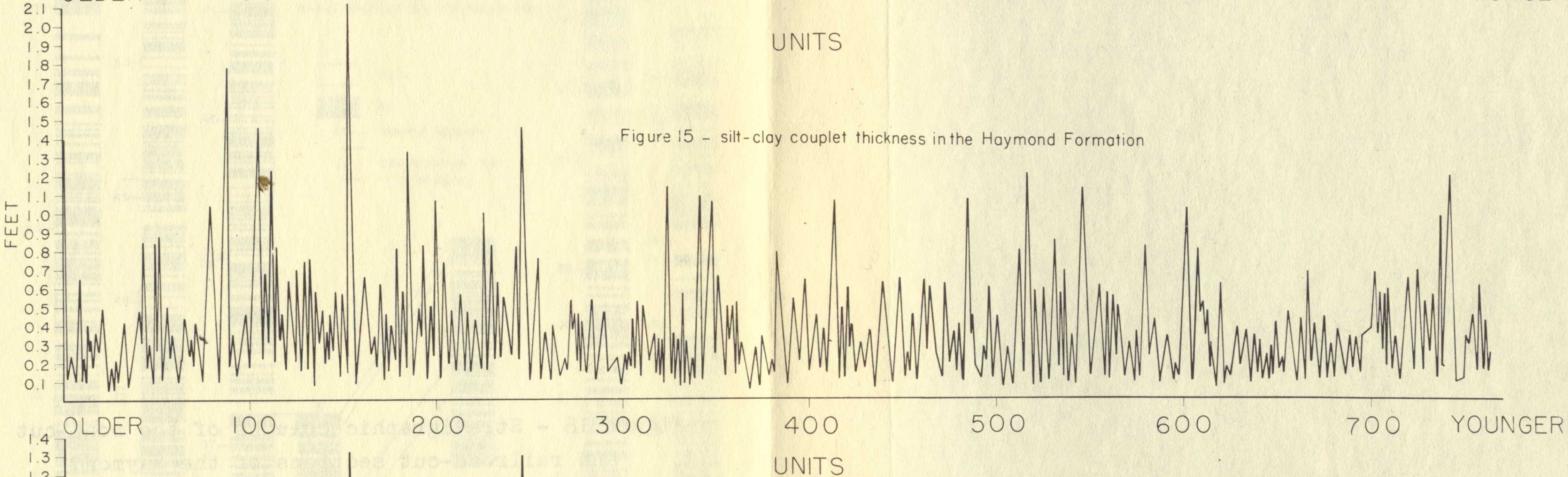

Figure 15 - silt-clay couplet thickness in the Haymond Formation

Figure 16 - silt layer thickness in the Haymond Formation

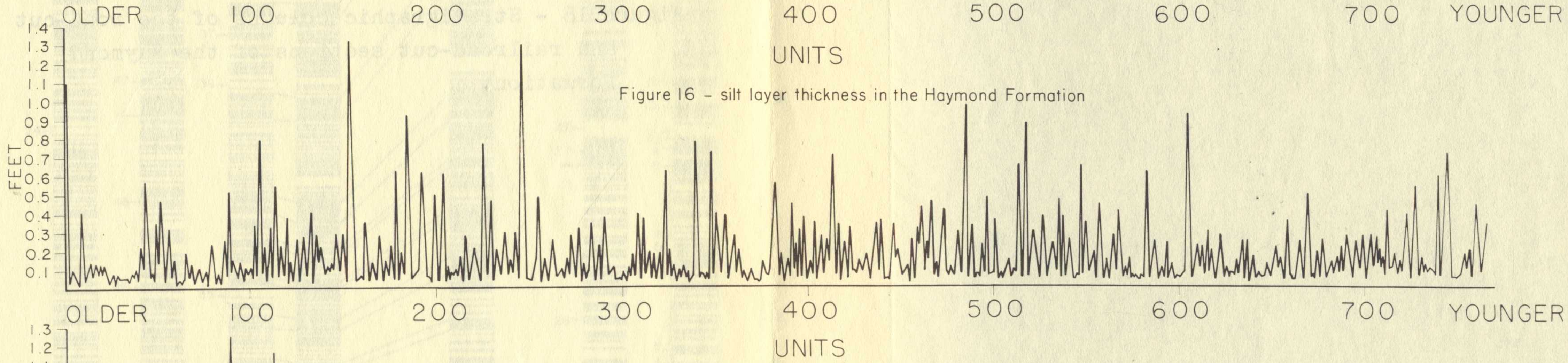

Figure 17 - clay layer thickness in the Haymond Formation

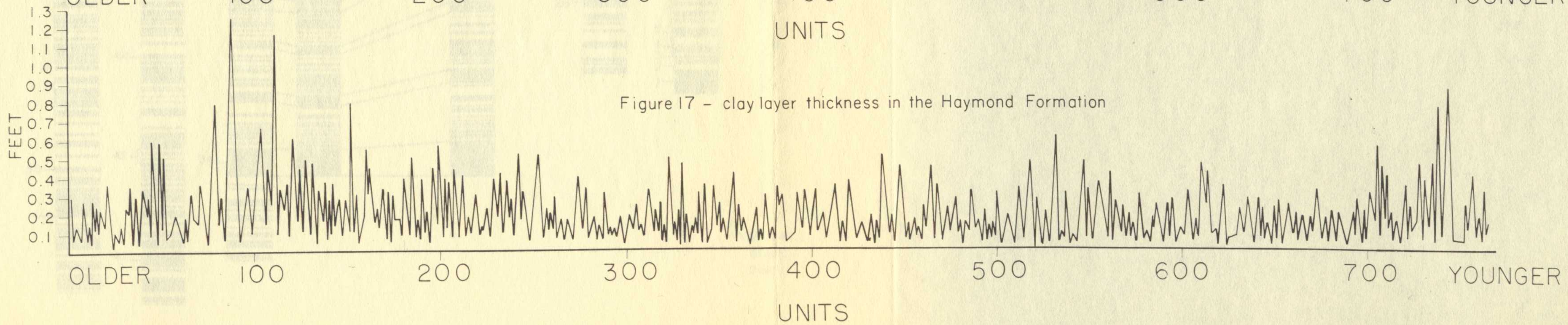

Figure 18 - Stratigraphic columns of the road-cut and railroad-cut sections of the Haymond Formation.

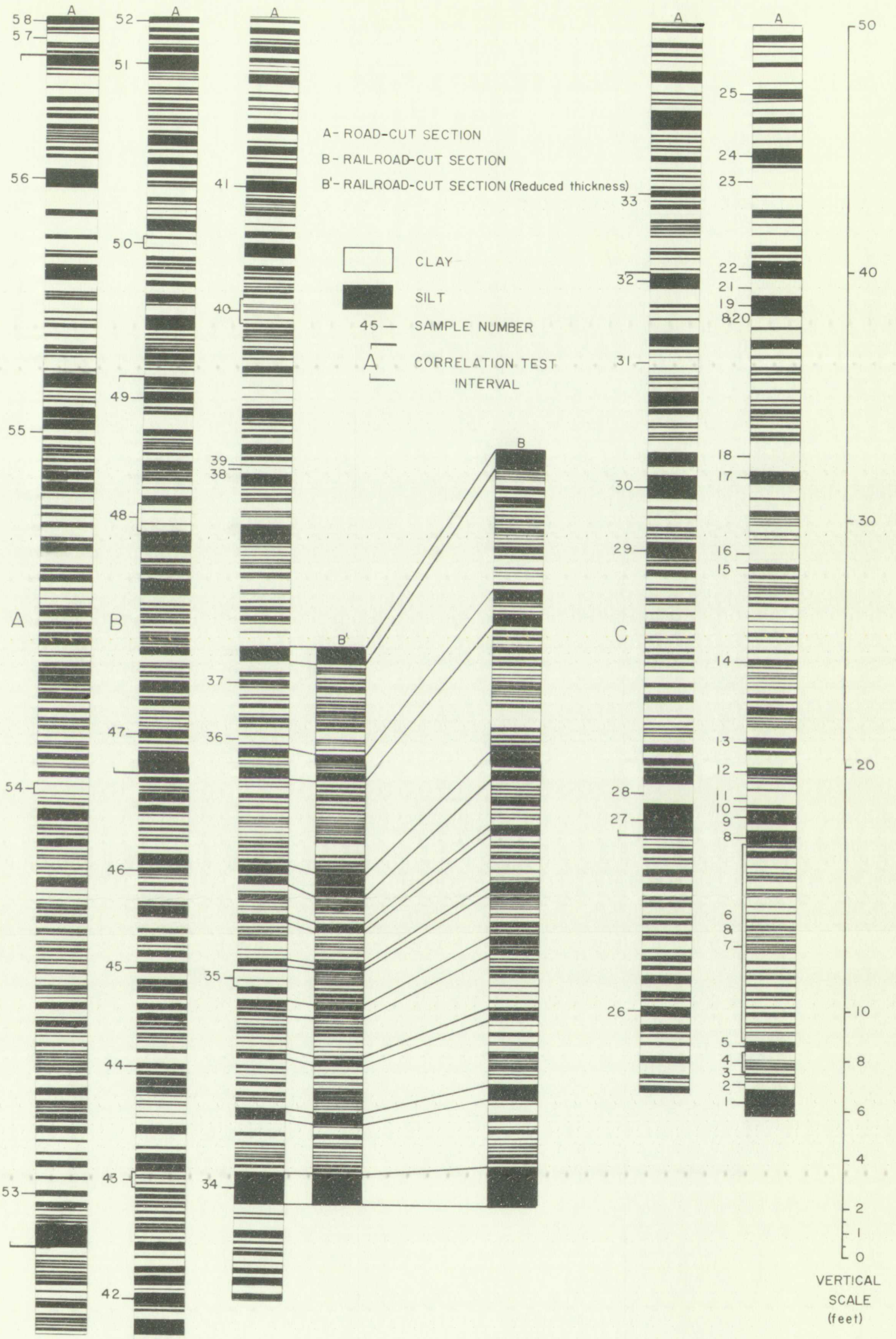
A- ROAD-CUT SECTION
B- RAILROAD-CUT SECTION
B'- RAILROAD-CUT SECTION (Reduced thickness)
CLAY
SILT
45 — SAMPLE NUMBER
CORRELATION TEST INTERVAL
A
B
C
B'
VERTICAL SCALE (feet)

left (Fig. 19). The siltstone thickness distributions are essentially the same for both the road-cut and railroad-cut sections with more than 75 percent of the layers less than 0.2 foot thick and modes in the 0.0 to 0.1 foot class interval. The shale thickness distributions are alike in that more than 75 percent of the layers are less than 0.2 foot thick but they differ in that the mode for the road-cut shale falls in the 0.1 to 0.2 foot class interval while the mode for the railroad-cut shale falls in the 0.0 to 0.1 foot class interval.

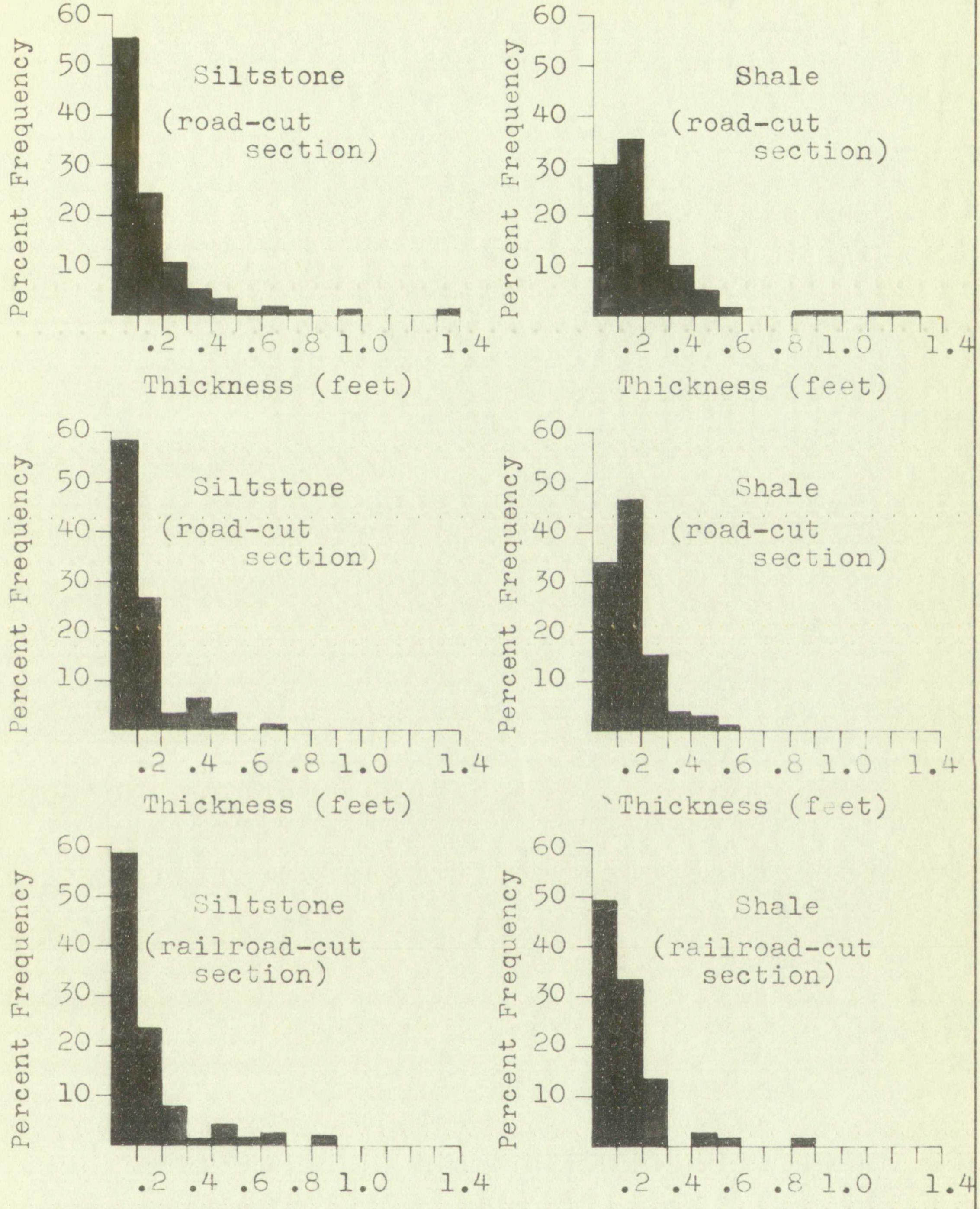

Figure 19 - Percent frequency of siltstone and shale thickness for the road-cut and railroad-cut sections of the Haymond Formation.

CORRELATION

The part of the Haymond Formation which crops out along the southern Pacific Railroad 2 miles east of Haymond station was correlated 8 miles in the field with part ofthe Haymond exposed in the road-cut in U. S. Highway 90 (Fig. 1). This field correlation was based on certain key beds and distinctive groups of beds (Figs. 2 and 3).

The individual layers of the railroad-cut section were plotted as a two component stratigraphic column to the correct scale in Figure 18 (column B). For better visual comparison, the section was reduced to 22 feet, the thickness of the assumed corresponding part of the road-cut section, by multiplying the thickness of each layer by 0.745. This reduced section is plotted as column B' in figure 18.

As the railroad-cut section contains more couplets than the corresponding part of the road-cut section, it was not possible to obtain a correlation coefficient using raw thickness data. As the thinner layers are probably the most variable laterally (see p. 40), all siltstone layers thinner than one standard deviation above the mean were grouped with the enclosing shale layers. Nine siltstone layers remained in both the railroad-cut section and the corresponding part of the road-cut section which, combined with the intervals between (shale plus siltstone layers less than the mean) gave 18 units in each section.

These 18 units were used to compute a correlation coefficient between the two sections of +0.998, almost perfect positive

correlation (Mills, 1955). This relatively objective, mathematical correlation indicates that the assumed field correlation was correct. To further strengthen this correlation, three other areas within the road-cut section were tested for correlation using the same procedure (Fig. 18, correlation test intervals A, B, and C). The following correlation coefficients were obtained: test interval A, +0.663; test interval B, +0.337; test interval C, +0.350. The assumed field correlation is thus further substantiated.

Lateral grading would be expected as a result of downslope size sorting, depositing relatively greater amounts of clay further downslope. Theoretically, a greater amount of silt would be deposited on the upper part of the slope so that any silt layer would thicken in an upslope direction. These lateral variations in size and thickness can be used to explain two features observed in the Haymond Formation. The first feature is the presence of silty claystone which has a composition between that of the siltstone and shale. Each silty claystone probably represents a thicker siltstone further upslope and a thinner shale layer downslope that is indistinguishable from the enclosing shale layers as a result of downslope decrease in grain size. The second feature is the combined upslope increase in: 1. the number of siltstone layers, 2. the thickness of the siltstone layers, and 3. the relative amount of silt. Based on paleocurrent analyses, the railroad-cut section of the Haymond Formation is upslope and to the south of the road-cut section (Fig. 1). Table 1 summarizes some of the silt-clay relationships between the road-cut section and

the railroad-cut section. As can be seen from the table, there is an increase in number and thickness of both silt and clay layers from the road-cut section to the railroad-cut section (upslope). However, the increase in clay is smaller, relative to the increase in silt, so that the amount of silt increases from 48 percent of the total thickness (silt:clay = 0.92) in the road-cut section to 52 percent of the total thickness (silt: clay = 1.07) in the railroad-cut section. These upslope increases are easily explained by lateral gradation resulting in a downslope increase in clay relative to silt.

Table 1: Upslope variation in silt and clay

SECTION	THICKNESS	NUMBER OF LAYERS	SILT:CLAY
Road-cut	22.37		0.92
silt	10.74	80	
clay	11.63	79	
Railroad-cut	30.31		1.07
silt	15.68	117	
clay	14.63	116	

ORIGIN OF STRATIFICATION

The siltstone-shale alternations of the Haymond Formation have many of the characteristics of geosynclinal sequences called "flysch". The Flysch Formation of the Alps is a Tertiary sequence over 10,000 feet thick, poor in fossils, and composed of interstratified marl, shale, and sandstone layers (Sujkowski, 1957). Van der Gracht (1931) described the Flysch as "a marine sequence of poorly fossiliferous clayey muds, with more or less sandy beds intercalated in shales, laid down to a great thickness". The term "flysch" has been applied, with slight variations in meaning, to similar sequences of different countries and ages. The term was first applied to the Haymond Formation by van der Gracht (1931).

According to Sujkowski (1957, p. 543), "flysch" sequences are characterized by great thicknesses of geosynclinal slope deposits, chiefly alternating marine shale and sandstone. Bokman (1953, p. 153) lists the following as characteristics of geosynclinal sediments: 1. great thicknesses of sediments, predominantly clastics, deposited in a relatively short period of time, 2. dark color, 3. scarcity of fossils, 4. rhythmic and/or graded shale and graywacke, and 5. presence of associated volcanics and radiolarites. Rich (1950 and 1951) calls such sequences slope or "clino" deposits characterized by bedding which is thin, persistent, and extremely even; alternating silt and clay; thinning downslope away from the edge of the shelf; features of downslope movement; and sparsity of fossils. He concludes that alternating silt and clay layers are the chief

characteristics of slope deposits. McBride (1962b, p. 47) reached the same conclusions for the Martinsburg Formation, an Ordovician "flysch" sequence in the central Appalachians.

Several lines of evidence suggest that the couplets of the Haymond Formation and similar sequences were deposited by storm-generated turbidity currents with an average frequency of 2 to 10 years. Riveroll and Jones (1954) report a strong 22.8 year double sunspot cycle in the varved Puente (Miocene) Formation of California which they attribute to storm activity. They also found a 7.5 year cycle similar to cycles widely reported in weather, tree ring, and varve thickness data. Hülsmann and Emery (1961) were able to calibrate turbidity current layers in recent sediments of the Santa Barbara basin, California using varves. Each of the diatom-detrital varve groups separating turbidity current layers contains 1 to 43 couplets with a mean of about 5 indicating an average of about 5 years between turbidity currents. A similar calibration was obtained by Anderson (report in preparation) for the Oligocene Florissant lake beds of Colorado where the normal diatomite-sapropel varve couplets are interrupted by graded turbidity layers on an average of every 4 or 5 years.

Studies on the characteristics of recent storms are currently being conducted by the Storm Surge Research Project of the U. S. Weather Bureau. A storm surge is defined as "the difference between the observed water level and that which would have been expected at the same place in the absence of the storm" (Harris, 1963, p. 2). The use of storm surge characteristics of storm-generated turbidites (1962), as well, reached the same conclusion for [illegible] interpreting an Ordovician "flysch" sequence in the central Appalachians.

Several lines of evidence suggest that the sequences of the Heyward Formation and similar sequences were deposited by storm-generated turbidity currents with an average frequency of 2 to 10 years. Rivereall and Jones (1954) recorded a 22.5 year double sunspot cycle in the varved [illegible] Formation of California which they attribute to storm activity. They also found a 7.5 year cycle similar to cycles widely reported in weather, tree rings, and varve thicknesses. Hülsemann and Emery (1961) were able to calibrate turbidity current layers in recent sediments of the Santa Barbara Basin of California using varves. Each of the diatom-detrital varve groups separating turbidity current layers contains 1 to 10 couplets with a mean of about 5 indicating an average of about 5 years between turbidity currents. A similar calibration was obtained by Anderson (personal communication) for the Eocene Florissant lake beds of Colorado where the normal diatomite-sapropel varve couplets are interrupted by graded detrital layers on an average of every 4 or 5 years.

Studies on the characteristics of recent storms are currently being conducted by the Storm Surge Research Project of the U. S. Weather Bureau. A storm surge is defined as "the difference between the observed water level and that which would have been expected at the same time in the absence of the storm" (Harris, 1963, p. 4). The use of [illegible] analyses eliminates the cycles caused by normal astronomic tides leaving only the effects on sea level caused by storms. Variations in monthly mean sea level and the corresponding storm surge charts for 3 U. S. Coast and Geodetic Survey tide stations on the Atlantic and Gulf coasts of the United States are shown in Figure 20. The storm surge data were computed by subtracting the normal sea level from the observed sea level (Harris, 1963, Fig. 0.3) for a particular month. The vertical lines superimposed on the storm surge charts represent sea level anomalies greater than two feet. The actual size of the anomaly is indicated wherever information was available. A summary of the frequency of these anomalies is given in Appendix VI for 17 U. S. Coast and Geodetic Survey tide stations along the Atlantic and Gulf coasts. Regional means range from 1.57 to 3.87 years between anomalies.

Assuming that the turbidity currents which deposited the silt layers of the Haymond Formation were generated by a storm process with a frequency of the same order of magnitude as the above examples, then each silt-clay couplet in the Haymond should represent a time interval of 2 to 5 years. Although every silt layer may be a record of a storm, there are several reasons why every storm would not be recorded by a silt layer. It is possible that several severe storms could have occurred within one year (Fig. 20) with insufficient time between storms for silt to accumulate. If we assume that the axes of structures presently exposed in the Marathon basin are parallel to the axis and edge of the Llanoria geosyncline, then the railroad-cut section of the Haymond Formation is 5 miles upslope from the

Figure 20 - Monthly mean observed sea level and storm surge at 3 selected Coast and Geodetic Survey tide stations. The year number is plotted on June. Marks indicate the occurrence of a storm which produced a tide anomaly as much as 2 feet at any hourly observation; the actual size of the anomaly is indicated by the figures wherever information was available (after Harris, 1963).

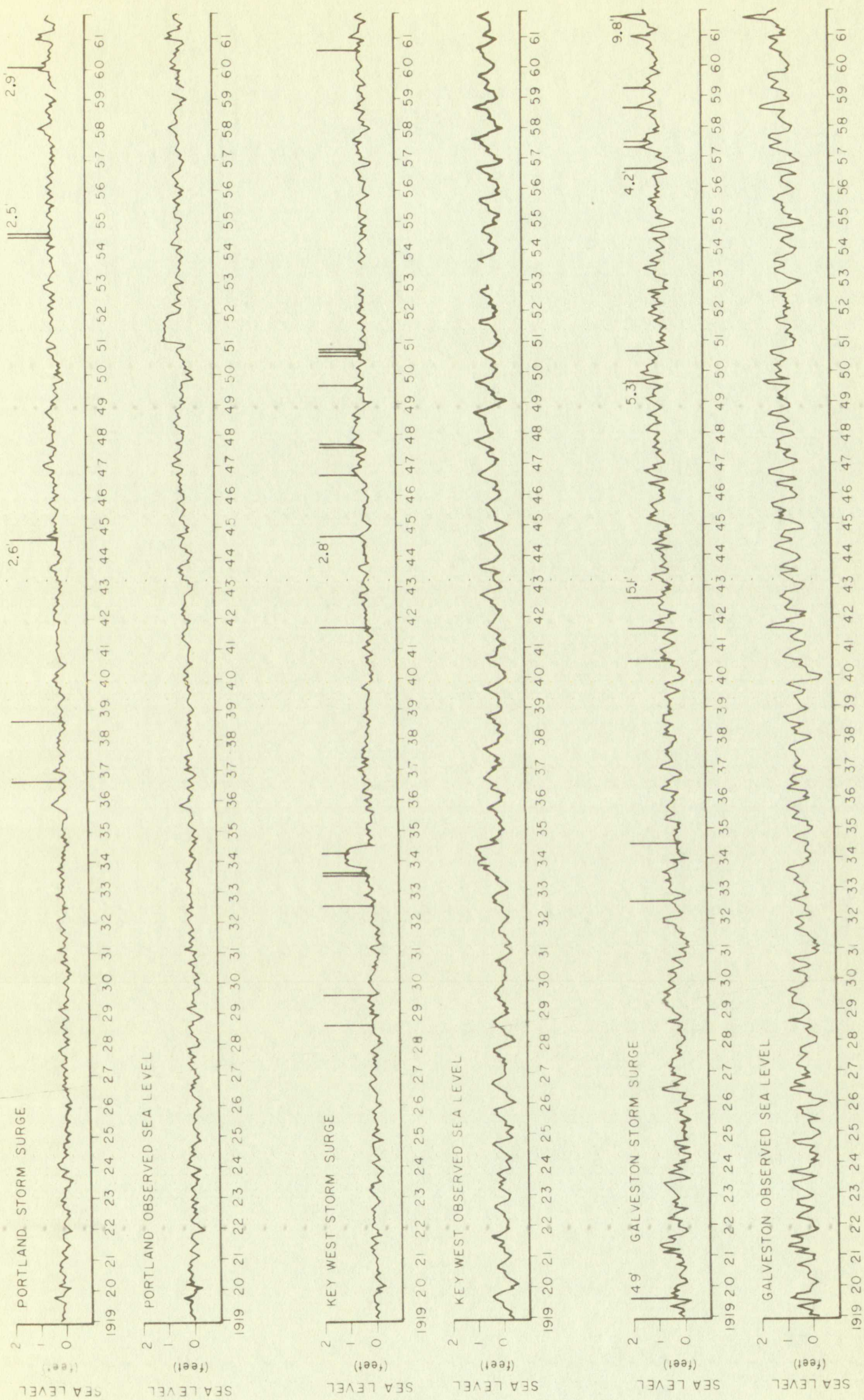

PORTLAND STORM SURGE
PORTLAND OBSERVED SEA LEVEL
KEY WEST STORM SURGE
KEY WEST OBSERVED SEA LEVEL
GALVESTON STORM SURGE
GALVESTON OBSERVED SEA LEVEL
SEA LEVEL (feet)
2
1
0
2.9'
2.5'
2.6'
2.8'
9.8'
4.2'
5.3'
5.1'
4.9'
1919 20 21 22 23 24 25 26 27 28 29 30 31 32 33 34 35 36 37 38 39 40 41 42 43 44 45 46 47 48 49 50 51 52 53 54 55 56 57 58 59 60 61
YEARS

road-cut section (distance corrected for folding and faulting). In this 5 miles, the number of silt layers has increased 46 percent. If we further assume that the siltstone layers in the railroad-cut section represent all storms capable of generating a turbidity current, then each siltstone layer in the railroad-cut section probably represents a time interval of 2 to 5 years and each siltstone in the road-cut probably represents a time interval of 4 to 10 years. These are minimum time intervals as the siltstone layers in the railroad-cut section probably represent only a fraction of the storms capable of generating a turbidity current.

CONCLUSIONS

.The silt-clay alternations of the Haymond Formation accumulated rapidly without important interruption on the slope of the Llanoria geosyncline. Paleocurrent and petrographic analyses indicate that the sediments were derived from an igneous and metamorphic terrane to the east. Each silt layer was deposited in a very short time by a turbidity current. The frequency of the turbidity currents was probably controlled by the storm frequency and availability of detrital material. Applying what is known about the characteristics of turbidity currents, the following sequence of events is suggested for the deposition of a typical silt-clay couplet in the Haymond Formation:

1. Silt and clay on the shelf were continually worked along the bottom by currents to the upper part of the slope. Waves and currents of a storm, stirred the accumulated sediments into suspension and generated a turbidity current which scoured and grooved the top surface of the underlying clay layer.

2. The turbidity current eventually lost momentum and the suspended material began to settle. At first, the settling was too rapid to permit size sorting. The current continued as laminar flow, reworking the silt and clay and redepositing them as cross laminations with a subparallel arrangement of platy and elongate grains. At this phase of laminar flow, scour-and-fill structures were formed by certain irregularities in flow. As the current continued to wane, slight changes in current velocity resulted in the periodic concentration of clay and plant fragments into horizontal micro-laminations.

3. Deformation of the cross and horizontal laminations into convolute folds occurred in the upper part of the silt layers in response to the downslope vector of gravity on the fluid silt mass.

4. After most of the current had passed, the remaining suspended clay and fine silt slowly settled to form a continuous sequence grading from silt to clay.

REFERENCES CITED

Bailey, E. B., 1930, Sedimentation in relation to tectonics: Geol. Soc. America Bull., v. 47, p. 1713-1726.

Bain, G. W., 1931, Flowage folding: Am. Jour. Sci., 5th ser., v. 22, p. 503-530.

Baker, C. L., 1932, Erratics and arkoses in the Middle Pennsylvanian Haymond Formation of the Marathon area, trans-Pecos Texas: Jour. Geology, v. 40, p. 577-607.

Baker, C. L. and Bowman, W. F., 1917, Geologic exploration of the southeastern Front Range of trans-Pecos Texas: Texas Univ. Bull. 1753, p. 61-172.

Baldry, R. A., 1938, On a theory of gravitational sliding applied to the Tertiary of Ancon, Ecuador: Geol. Soc. London Quart. Jour., v. 94, p. 359-370.

Beets, C., 1946, Miocene submarine disturbances of strata in northern Italy: Jour. Geology, v. 54, p. 229-245.

Billings, M. P., 1954, Structural geology: New York, Prentice-Hall, Inc., 514 p.

Bisque, R. E., 1961, Analysis of carbonate rocks for calcium, magnesium, iron and aluminum with EDTA: Jour. Sedimentary Petrology, v. 31, p. 113-122.

Bokman, J., 1953, Lithology and petrology of the Stanley and Jackfork Formations: Jour. Geology, v. 61, p. 152-170.

Calvert, S. E. and Veevers, J. J., 1962, Minor structures of unconsolidated marine sediments revealed by X-radiography: Sedimentology, v. 1, p. 287-295.

Carney, F., 1935, Glacial beds of Pennsylvanian age in Texas (abstract): Geol. Soc. America Proc. for 1934, p. 70.

Cheney, M. G., 1929, Stratigraphic and structural studies in north-central Texas: Texas Univ. Bull. 2913, 27 p.

Clarke, J. M., 1918, Strand and undertow markings of Upper Devonian time as indications of the prevailing climate: New York State Mus. Bull. 196, p. 199-238.

Cline, L. M., 1960, Late Paleozoic rocks of the Ouachita Mountains: Oklahoma Geol. Survey Bull. 85, 113 p.

Cope. F. W., 1946, Intraformational contorted rocks in the upper Carboniferous of the southern Pennines: Geol. Soc. London Quart. Jour., v. 101, p. 139-176.

Crowell, J. C., 1955, Directional current structures from pre-Alpine Flysch, Switzerland: Geol. Soc. America Bull. v. 66, p. 1351-1384.

----- 1958, Sole markings of graded graywacke beds; a discussion: Jour. Geology, v. 66, p. 333-335.

Dott, R. H. and Howard, J. K., 1962, Convolute laminations in non-graded sequences: Jour. Geology, v. 70, p. 114-121.

Dunbar, C. O., 1960, Historical geology: New York, John Wiley and Sons, Inc., 500 p.

Flawn, P. T., 1958, Genesis of Haymond boulder beds; discussion: Am. Assoc. Petroleum Geologists Bull., v. 42, p. 1734-1735.

Glaessner, M. F., 1958, Sedimentary flow structures on bedding planes: Jour. Geology, v. 66, p. 1-7.

Greensmith, J. T., 1956, Sedimentary structures in the upper Carboniferous of north and central Derbyshire: Jour. Sedimentary Petrology, v. 26, p. 343-355.

Grim, R. E., 1953, Clay mineralogy: New York, McGraw-Hill Book Company, Inc., 384 p.

Haaf, E. ten, 1956, Signigicance of convolute lamination: Geol. en Mijnbouw, v. 18, p, 188-194.

Hall, W. E., 1956, Marathon folded belt in Big Bend area of Texas: Am. Assoc. Petroleum Geologists Bull., v.40, p. 2247-2255.

----- 1957, Genesis of Haymond boulder beds, Marathon basin, west Texas: Am. Assoc. Petroleum Geologists Bull., v. 41, p. 1633-1637.

----- 1959, Genesis of "Haymond boulder beds," Marathon basin, west Texas; discussion: Am. Assoc. Petroleum Geologists Bull., v. 43, p. 238-239.

Hamblin, W. K., 1962a, Staining and etching techniques for studying obscure structures in clastic rocks: Jour. Sedimentary Petrology, v. 32, p. 530-533.

----- 1962b, X-radiography in the study of structures in homogeneous sediments: Jour. Sedimentary Petrology, v. 32, p. 201-210.

Harris, D. L., 1963, Characteristics of the hurricane storm surge: U.S. Weather Bur. Tech. Paper 48, 139 p.

Holland, C. H., 1960, Load cast terminology and origin of convolute bedding; some comments: Geol. Soc. America Bull., v. 71, p. 633.

Hsu, K. J., 1958, Paleocurrent structures in Ultrahelvetic Flysch of Swiss Alps and their paleogeographic and paleotectonic signigicances (abstract): Geol. Soc. America Bull., v. 69, p. 1588-1589.

----- 1959, Flute-and groove-casts in the pre-Alpine Flysch, Switzerland: Am. Jour. Sci., 5th ser., v. 257, p. 529-536.

Hülsmann, J. and Emery, K. O., 1961, Stratification in recent sediments of Santa Barbara basin as controlled by organisms and water character: Jour. Geology, V. 69, p. 279-290.

Johnson, K. E., 1962, Paleocurrent study of the Tesnus Formation, Marathon basin, Texas: Jour. Sedimentary Petrology, v. 32, p. 781-792.

Jones, O. T., 1937, On the sliding of slumping of submarine sediments in Denbighshire, North Wales, during the Ludlow Period: Geol. Soc. London Quart. Jourl, v. 93, p. 241-283.

Kelling, G. and Walton, E. K., 1957, Load cast structures; their relationship to upper surface structures and their mode of formation: Geol. Mag., v. 94, p. 481-490.

Kerr, P. F., 1959, Optical mineralogy: New York, McGraw-Hill Book Company, Inc., 442 p.

----- 19[illegible], [illegible] west Texas [illegible]: Am. Assoc. Petroleum Geologists Bull., v. [illegible], p. 2[illegible].

Hamblin, W. K., 1962a, Staining and etching techniques for studying obscure structures in clastic rocks: Jour. Sedimentary Petrology, v. 32, p. 530-533.

----- 1962b, X-ray radiography in the study of structures in homogeneous sediments: Jour. Sedimentary Petrology, v. 32, p. 201-210.

Harris, D. L., 1963, Characteristics of the hurricane storm surge: U.S. Weather Bur. Tech. Paper 48, 139 p.

Holland, C. H., 1960, Load cast terminology and origin of convolute bedding: some comments: Geol. Soc. America Bull., v. 71, p. 655.

Hsu, K. J., 1958, Paleocurrent structures in the Molasse and Flysch of Swiss Alps and their paleogeographic and paleotectonic significance (abstract): Geol. Soc. America Bull., v. 69, p. 1588-1589.

----- 1959, Flute-and groove-casts in the pre-alpine flysch, Switzerland: Am. Jour. Sci., 5th ser., v. 257, p. 529-536.

Hulsemann, J., and Emery, K. O., 1961, Stratification in recent sediments of Santa Barbara basin as controlled by organisms and water character: Jour. Geology, v. 69, p. 279-290.

Johnson, K. G., 1962, Paleocurrent study of the Tesnus Formation, Marathon basin, Texas: Jour. Sedimentary Petrology, v. 32, p. 781-792.

Jones, O. T., 1937, On the sliding or slumping of submarine sediments in Denbighshire, North Wales, during the Ludlow Period: Geol. Soc. London Quart. Jour., v. 93, p. 241-283.

Kelling, G., and Walton, E. K., 1957, Load-cast structures: their relationship to upper-surface structures and their mode of formation: Geol. Mag., v. 94, p. 481-490.

Kerr, P. F., 1959, Optical mineralogy: New York, McGraw-Hill Book Co., [illegible] p.

Kindle, E. M., 1917, Deformation of unconsolidated beds in Nova Scotia and southern Onterio: Am. Assoc. Petroleum Geologists Bull., v. 28, p. 323-334.

King, P. B., 1930, Geology of the Glass Mountains; Part 1, descriptive geology: Texas Univ. Bull. 3038, 166 p.

----- 1937, Geology of the Marathon region, Texas: U.S. Geol. Survey Prof. Paper 187, 148 p.

----- 1958, Problems of boulder beds of Haymond Formation, Marathon basin, Texas: Am. Assoc. Petroleum Geologists Bull., v. 42, p. 1731-1734.

King, P. B. and King, R. E., 1928, The Pennsylvanian and Permian stratigraphy of the Glass Mountains: Texas Univ. Bull. 2801, p. 109-145.

Kuenen, Ph. H., 1949, Slumping in the Carboniferous rocks of Pembrokeshire: Geol. Soc. London Quart. Jour., v. 104, p.365-385.

----- 1953, Significant features of graded bedding: Am. Assoc. Petroleum Geologists Bull., v. 37, p. 1044-1066.

----- 1957, Sole markings of graded graywacke beds: Jour. Geology, v. 65, p. 231-258.

Kuenen, Ph. H. and Carozzi, A., 1953, Turbidity currents and sliding in geosynclinal basins in the Alps: Jour. Geology, v. 61, p. 363-372.

Kuenen, Ph. H. and Menard, H. W., 1952, Turbidity currents, graded and nongraded deposits: Jour. Sedimentary Petrology, v. 22, p. 83-96.

Kuenen, Ph. H. and Migliorini, G. I., 1950, Turbidity currents as a cause of graded bedding: Jour. Geology, v. 58, p. 91-126.

Kuenen, Ph. H. and Prentice, J. E., 1957, Flow-markings and load-casts: Geol. Mag., vol. 94, p. 173-174.

[illegible], E. R., 1949, Deformation [illegible] New Mexico and [illegible]: Am. Assoc. Petroleum Geologists Bull., v. 26, p. [illegible].

King, P. B., 1930, Geology of the Glass Mountains, Texas, pt. 1, descriptive geology: Texas Univ. Bull. 3038, 167 p.

----- 1937, Geology of the Marathon region, Texas: U.S. Geol. Survey Prof. Paper 187, 148 p.

----- 1958, Problems of boulder beds of Haymond Formation, Marathon basin, Texas: Am. Assoc. Petroleum Geologists Bull., v. 42, p. 1731-1735.

King, P. B. and King, R. E., 1928, The Pennsylvanian and Permian stratigraphy of the Glass Mountains: Texas Univ. Bull. 2801, p. 109-145.

Kuenen, Ph. H., 1948, Slumping in the Carboniferous rocks of Pembrokeshire: Geol. Soc. London Quart. Jour., v. 104, p. 365-385.

----- 1953, Significant features of graded bedding: Am. Assoc. Petroleum Geologists Bull., v. 37, p. 1044-1066.

----- 1957, Sole markings of graded graywacke beds: Jour. Geology, v. 65, p. 231-258.

Kuenen, Ph. H. and Carozzi, A., 1953, Turbidity currents and sliding in geosynclinal basins of the Alps: Jour. Geology, v. 61, p. 363-373.

Kuenen, Ph. H. and Menard, H. W., 1952, Turbidity currents, graded and nongraded deposits: Jour. Sedimentary Petrology, v. 22, p. 83-96.

Kuenen, Ph. H. and Migliorini, C. I., 1950, Turbidity currents as a cause of graded bedding: Jour. Geology, v. 58, p. 91-125.

Kuenen, Ph. H. and Prentice, J. E., 1957, Flow-markings and load-casts: Geol. Mag., v. 94, p. 173-174.

Kuenen, Ph. H. and Sanders, J., 1956, Sedimentation phenomena in Kulm and Flötzleeres Graywackes, Sauerland and Oberharz, Germany: Am. Jour. Sci., 5th ser., v. 254, p. 649-671.

Kuenen, Ph. H. and Ten Haaf, E., 1958, Sole markings of graded graywacke beds; a reply: Jour. Geology, v. 66, p. 335-337.

Lamont, A., 1938, "Contemporaneous slumping and other problems at Bray Series, Ordovician, and lower Carboniferous horizons, in County Doublin: Royal Irish Acad. Proc., v. 45, p. 1-32.

McBride, E. F., 1962a, Flysch and associated beds of the Martinsburg Formation (Ordovician), central Appalachians: Jour. Sedimentary Petrology, v. 32, p. 39-91.

----- 1962b, Sedimentology of the Haymond Formation (Pennsylvanian flysch), Marathon basin, Texas (abstract): Geol. Soc. America Sp. Paper 73, p. 204.

Mills, F. C., 1955, Statistical methods: Now York, Henry Holt and Company, 746 p.

Miser, H. D., and Hendricks, T. A., 1960, Age of Johns Valley Shale, Jackfork Sandstone, and Stanley Shale: Am. Assoc. Petroleum Geologists Bull., v. 44, p. 1829-1834.

Miser, H. D. and Sellards, E. H., 1931, Pre-Cretaceous rocks found in wells in Gulf Coastal Plain south of Ouachita Mountains: Am. Assoc. Petroleum Geologists Bull., v. 15, p. 801-818.

Moore, R. C., 1929, Correlation of Pennsylvanian formations of Texas and Oklahoma: Am. Assoc. Petroleum Geologists Bull., v. 13, p. 883-902.

Pantin, H. M., 1960, Dye-staining technique for examination of sedimentary microstructures in cores: Jour. Sedimentary Petrology, v. 30, p. 314-316.

Pettijohn, F. J., 1957, Sedimentary rocks: New York, Harper and Brothers, 718 p.

Plummer, F. B., 1931, Pennsylvanian sedimentation in Texas: Illinois Geol. Survey Bull. 60, p. 259-269.

Plummer, F. B. and Moore, R. C., 1921, Stratigraphy of the Pennsylvanian formations of north-central Texas: Texas Univ. Bull. 2132, 237 p.

Powers, S., 1928, Age of folding of the Oklahoma Mountains; the Ouachita, Arbuckle, and Wichita Mountains of Oklahoma and the Llano-Burnet and Marathon Uplifts of Texas: Geol. Soc. America Bull., v. 39, p. 1030-1072.

Prentice, J. E., 1956, The interpretation of flow markings and load casts: Geol. Mag., v. 93, p. 393-400.

----- 1960, Flow structures in sedimentary rocks: Jour. Geology, v. 58, p. 217-225.

Rettger, R. E., 1935, Experiments in soft rock deformation: Am. Assoc. Petroleum Geologists Bull., v. 19, p. 271-290.

Rich, J. L., 1950, Flow markings, groovings, and intra-stratal crumplings as criteria for the recognition of slope deposits, with illustrations from Silurian rocks of Wales: Am. Assoc. Petroleum Geologists Bull., v. 34, p. 717-741.

----- 1951, Three critical environments of deposition and criteria for recognition of rocks deposited in each of them: Geol. Soc. America Bull., v. 62, p. 1-19.

Rich, J. L. and Wilson, W.J., 1950, Paleogeographic and stratigraphic significance of subaqueous flow markings in the Lower Mississippian strata of south-central Ohio and adjacent parts of Kentucky (abstract): Geol. Soc. America Bull., v. 61, p. 1496.

Richter, R., 1935, Marken und Spuren im Hunsrück-Schiefer; I, Gefliess-Marken: Senckenberg. Naturf. Gesell. Abh., v. 17, p. 244-263.

Riveroll, D. D. and Jones, B. C., 1954, Varves and foraminifera of a portion of the upper Puente Formation (upper Miocene), Puente, California: Jour. Paleontology, v. 28, p. 121-131.

Rücklin, H., 1938, Strömungs-Marken im unteren Muschelkalk des Saarlandes: Senckenberg. Naturf. Gesell. Abh., v. 20, p. 94-114.

Plummer, F. B. and Moore, R. C., 1921, Stratigraphy of the Pennsylvanian formations of north-central Texas: Texas Univ. Bull. 2132, 237 p.

Powers, S., 1928, Age of folding of the Oklahoma Mountains: the Ouachita, Arbuckle, and Wichita Mountains of Oklahoma and the Llano-Burnet and Marathon uplifts of Texas: Geol. Soc. America Bull., v. 39, p. 1031-1072.

Prentice, J. E., 1956, The interpretation of flow markings and load casts: Geol. Mag., v. 93, p. 393-400.

----- 1960, Flow structures in sedimentary rocks: Jour. Geology, v. 68, p. 217-225.

Rettger, R. E., 1935, Experiments in soft rock deformation: Am. Assoc. Petroleum Geologists Bull., v. 19, p. 271-290.

Rich, J. L., 1950, Flow markings, groovings, and intra-stratal crumplings as criteria for the recognition of slope deposits, with illustrations from Silurian rocks of Wales: Am. Assoc. Petroleum Geologists Bull., v. 34, p. 717-741.

----- 1951, Three critical environments of deposition and criteria for recognition of rocks deposited in each of them: Geol. Soc. America Bull., v. 62, p. 1-19.

----- and Wilson, E. J., 1950, Paleogeographic and stratigraphic significance of subaqueous flow markings in the lower Mississippian strata of south-central Ohio and adjacent parts of Kentucky (abstract): Geol. Soc. America Bull., v. 61, p. 1496.

Richter, R., 1935, Marken und Spuren im Hunsrück-Schiefer: I, Gefliess-Marken: Senckenberg. Naturf. Gesell. Abh., v. 17, p. 244-263.

Riverll, D. D. and Jones, D. C., 1954, Varves and foraminifera of a portion of the upper Puente Formation (upper Miocene), Puente, California: Jour. Paleontology, v. 28, p. 121-131.

Rücklin, H., 1938, Strömungs-Marken im unteren Muschelkalk des Saarlandes: Senckenberg. Naturf. Gesell. Abh., v. 20, p. 94-114.

Sanders, J. E., 1960, Origin of convolute laminae: Geol. Mag., v. 97, p. 409-421.

Sellards, E. H., Adkins, W. S., and Plummer, F. B., 1932, The geology of Texas; vol. 1, stratigraphy: Texas Univ. Bull. 3232, p. 117-127.

Shrock, R. R., 1948, Sequences in layered rocks: New York, McGraw-Hill Book Company, Inc., 507 p.

Stewart, H. B., 1956, Contorted sediments in modern coastal lagoon explained by laboratory experiments: Am. Assoc. Petroleum Geologists Bull., v. 40, p. 153-179.

Sujkowski, Z. C., 1957, Flysch sedimentation: Geol. Soc. America Bull., v. 68, p. 543-554.

Sullwold, H. H., Jr., 1959, Nomenclature of load deformation in turbidites: Geol. Soc. America Bull., v. 70, p. 1247-1248.

Udden, J. A., Baker, C. L., and Bose, E., 1916, Review of the Geology of Texas: Texas Univ. Bull. 44, 164 p.

Van der Gracht, W. A. J. M. van Waterschoot, 1931, Permo-Carboniferous orogeny in south-central United States: Am. Assoc. Petroleum Geologists Bull., v. 15, p. 991-1057.

Williams, E., 1960, Intra-stratal flow and convolute folding: Geol. Mag., v. 97, p. 208-214.

Sanders, J. E., 1960, Origin of convolute laminae: Geol. Mag., v. 97, p. 409-421.

Sellards, E. H., Adkins, W. S., and Plummer, F. B., 1932, The geology of Texas, vol. 1, stratigraphy: Texas Univ. Bull. 3232, p. 117-127.

Shrock, R. R., 1948, Sequences in layered rocks: New York, McGraw-Hill Book Company, Inc., 507 p.

Stewart, H. B., 1956, Contorted sediments in modern coastal lagoon explained by laboratory experiments: Am. Assoc. Petroleum Geologists Bull., v. 40, p. 153-179.

Sujkowski, Z. L., 1957, Flysch sedimentation: Geol. Soc. America Bull., v. 68, p. 543-554.

Sullwold, H. H., Jr., 1959, Nomenclature of load deformation in turbidites: Geol. Soc. America Bull., v. 70, p. 1247-1248.

Udden, J. A., Baker, C. L., and Bose, E., 1916, Review of the Geology of Texas: Texas Univ. Bull. 44, 164 p.

Van der Gracht, W. A. J. M. Van Waterschoot, 1931, Permo-Carboniferous orogeny in south-central United States: Am. Assoc. Petroleum Geologists Bull., v. 15, p. 991-1057.

Williams, E., 1960, Intra-stratal flow and convolute folding: Geol. Mag., v. 97, p. 208-214.

APPENDIX I

Summary of the mineralogic composition of 18 samples from the Haymond Formation. Percentages were estimated from thin sections.

tr. = one grain observed
-1 = more than one grain but less than 1 percent observed

SAMPLE #	QUARTZ	ALBITE	GARNET	MUSCOVITE	BIOTITE	CLAY	PLANT FRAGMENTS
Siltstone:							
5	67	-1	-1	1	tr.	26	5
12	72	1	2	3	tr.	20	2
26	66	2	1	3	1	25	2
30	73	-1	-1	-1	tr.	23	2
37	73	-1	1	2	tr.	20	3
47	70	-1	-1	2	tr.	20	7
52	73	-1	-1	-1	tr.	23	2
56	70	1	1	3	tr.	20	5
Silty Claystone:							
11	70	-1	-1	5	tr.	60	6
18	25	1	1	1	tr.	60	12
36	45	4	3	2	1	25	20
40	40	2	1	1	tr.	46	10
48	25	-1	1	5	tr.	60	8
Shale:							
11	20	-1	1	8	tr.	69	2
18	10	-1	2	3	tr.	82	3
36	10	-1	3	3	tr.	80	4
40	15	-1	4	8	tr.	67	5
48	15	-1	2	5	tr.	75	3

APPENDIX II

Determination of organic (Kjeldahl) nitrogen, $CaCO_3$, $MgCO_3$, and total iron in the measured road-cut section of the Haymond Formation.

nd = no determination made
tr. = trace

SAMPLE	LITHOLOGY	% N x 10^{-3} (Kjeldahl)	% $CaCO_3$	% $MgCO_3$	% Fe^{+3}
1	siltstone	1.8	nd	nd	nd
2	shale	2.3	nd	nd	nd
5	siltstone	1.5	2.8	0.2	2.9
8	siltstone	2.2	nd	nd	nd
10	siltstone	3.0	nd	nd	nd
11	shale	2.6	4.6	0.2	3.1
12	siltstone	1.8	1.7	0.6	3.6
13	siltstone	2.0	nd	nd	nd
14	siltstone	1.3	nd	nd	nd
16	shale	2.8	nd	nd	nd
17	siltstone	1.4	nd	nd	nd
18	shale	3.0	4.2	tr.	3.4
19	shale	4.0	nd	nd	nd
21	shale	2.7	nd	nd	nd
22	siltstone	1.4	nd	nd	nd
23	shale	2.8	nd	nd	nd
24	siltstone	1.0	nd	nd	nd
25	siltstone	2.7	nd	nd	nd
26	siltstone	1.4	2.5	0.3	2.7
27	siltstone	1.6	nd	nd	nd
28	shale	2.5	5.2	0.6	3.0
29	siltstone	1.7	nd	nd	nd
31	shale	1.4	nd	nd	nd
33	siltstone	2.0	nd	nd	nd
34	siltstone	2.4	nd	nd	nd
35	shale	2.2	nd	nd	nd
36	shale	2.0	3.6	0.4	3.5

SAMPLE	LITHOLOGY	% N x 10^{-3} (Kjeldahl)	% $CaCO_3$	% $MgCO_3$	% Fe^{+3}
37	siltstone	2.0	0.9	0.4	3.4
38	shale	1.7	nd	nd	nd
40	shale	3.0	5.0	0.1	3.0
41	siltstone	2.2	nd	nd	nd
43	shale	1.4	3.8	tr.	3.3
44	siltstone	3.0	nd	nd	nd
45	siltstone	1.6	nd	nd	nd
47	siltstone	3.1	1.2	tr.	2.7
48	shale	1.4	4.9	tr.	2.9
49	siltstone	2.0	nd	nd	nd
50	shale	1.9	nd	nd	nd
51	siltstone	3.6	nd	nd	nd
52	siltstone	nd	1.2	0.1	3.0
54	shale	1.0	nd	nd	nd
56	siltstone	3.1	2.8	1.0	3.6
57	shale	nd	11.7	0.2	2.9

APPENDIX III

Summary of flute and groove cast measurements on the bottom surfaces of silt beds of the Haymond Formation.

ns = no sample collected

SAMPLE	BED THICKNESS (feet)	NUMBER OF MEASUREMENTS	MEAN AZIMUTH (o)	SPREAD (o)
1	1.10	3	92	10
5	0.41	6	82	28
8	0.57	12	80	29
12	0.35	3	86	29
13	0.47	1	96	-
14	0.19	3	73	23
ns	0.26	3	78	23
ns	0.34	6	82	21
22	0.69	3	76	31
ns	0.33	3	96	24
24	0.55	2	92	11
ns	0.29	1	58	-
ns	0.29	1	72	-
27	1.32	1	71	-
ns	0.66	1	95	-
ns	0.31	2	80	18
29	0.63	3	81	18
30	0.94	5	65	21
ns	0.55	4	94	55
ns	0.50	4	91	12
32	0.61	10	80	21
33	0.28	4	82	19
ns	0.21	3	81	9
ns	0.77	6	70	22
ns	0.46	4	76	17
ns	0.13	2	97	14
ns	0.30	5	69	12
ns	0.09	2	90	11

SAMPLE	BED THICKNESS (feet)	NUMBER OF MEASUREMENTS	MEAN AZIMUTH (o)	SPREAD (o)
ns	0.30	3	81	7
34	1.30	20	80	17
ns	0.48	3	85	26
ns	0.16	1	73	-
ns	0.26	3	92	19
ns	0.28	2	79	11
ns	0.38	7	85	27
ns	0.40	2	84	9
ns	0.63	6	89	7
ns	0.20	3	83	9
ns	0.72	1	92	-
ns	0.13	2	88	8
ns	0.39	2	89	-
ns	0.28	2	98	16
ns	0.20	3	82	25
ns	0.14	1	84	-
ns	0.11	1	63	-
ns	0.56	8	89	30
ns	0.15	2	88	8
ns	0.23	1	85	-
ns	0.31	3	111	3
ns	0.38	2	79	5
ns	0.45	3	95	19
ns	0.28	3	88	27
ns	0.27	2	67	7
42	0.34	7	84	20
ns	0.24	1	80	-
ns	0.23	2	81	2
ns	0.32	4	103	31
ns	0.35	3	95	20
ns	0.36	2	79	10
ns	0.57	7	100	35
ns	0.10	3	96	9
ns	0.10	2	66	12
ns	0.32	6	85	31

SAMPLE	BED THICKNESS (feet)	NUMBER OF MEASUREMENTS	MEAN AZIMUTH (o)	SPREAD (o)
45	0.43	4	75	11
ns	0.24	2	86	1
ns	0.46	3	71	18
46	0.21	2	88	42
ns	0.42	3	79	24
ns	0.25	4	92	11
ns	0.30	2	94	15
ns	0.97	2	94	12
47	0.33	1	78	-
ns	0.23	1	100	-
ns	0.09	2	83	16
ns	0.36	4	85	24
ns	0.65	4	73	29
ns	0.30	4	85	15
ns	0.88	1	80	-
ns	0.30	3	114	31
ns	0.38	3	77	25
ns	0.38	3	125	6
ns	0.37	6	89	32
ns	0.65	3	79	22
ns	0.20	3	89	21
ns	0.45	4	82	8
ns	0.15	2	98	37
ns	0.09	2	85	6
ns	0.28	5	100	16
ns	0.27	5	92	19
ns	0.41	3	88	10
ns	0.16	1	106	-
51	0.69	3	92	5
52	0.25	5	96	12
ns	0.24	1	90	-
ns	0.93	2	89	-
53	0.23	4	101	8
ns	0.27	3	99	17
ns	0.25	3	84	18

SAMPLE	BED THICKNESS (feet)	NUMBER OF MEASUREMENTS	MEAN AZIMUTH (°)	SPREAD (°)
ns	0.50	4	83	21
ns	0.27	2	97	16
ns	0.38	2	83	11
ns	0.40	2	65	4
ns	0.54	4	83	20
ns	0.60	3	80	6
56	0.72	2	73	21
ns	0.44	1	97	-
58	0.34	3	86	20

APPENDIX IV

Silt, clay and total couplet thickness (in feet) of the road-cut section of the Haymond Formation.

silt	clay	couplet	silt	clay	couplet	silt	clay	couplet
1.10	0.30	1.40	0.05	0.05	0.10	0.15	0.20	0.35
0.05	0.07	0.12	0.06	0.15	0.21	0.05	0.16	0.21
0.03	0.07	0.12	0.06	0.24	0.30	0.02	0.16	0.18
0.03	0.11	0.14	0.06	0.21	0.27	0.04	0.08	0.12
0.10	0.14	0.24	0.06	0.36	0.42	0.04	0.06	0.10
0.07	0.13	0.20	0.04	0.04	0.08	0.03	0.19	0.27
0.05	0.08	0.13	0.05	0.08	0.13	0.05	0.07	0.12
0.03	0.07	0.10	0.08	0.30	0.38	0.19	0.25	0.44
0.02	0.28	0.30	0.06	0.05	0.11	0.06	0.31	0.37
0.41	0.24	0.65	0.10	0.08	0.18	0.07	0.59	0.66
0.04	0.07	0.11	0.04	0.22	0.26	0.52	1.26	1.78
0.07	0.15	0.22	0.07	0.34	0.41	0.09	0.10	0.19
0.05	0.05	0.10	0.22	0.26	0.48	0.15	0.20	0.35
0.12	0.28	0.40	0.11	0.20	0.31	0.10	0.19	0.29
0.14	0.13	0.27	0.57	0.28	0.85	0.07	0.06	0.13
0.07	0.25	0.32	0.12	0.09	0.21	0.06	0.14	0.20
0.07	0.11	0.18	0.12	0.60	0.72	0.14	0.14	0.28
0.13	0.23	0.36	0.06	0.24	0.30	0.09	0.12	0.21
0.08	0.19	0.27	0.08	0.12	0.20	0.04	0.28	0.32
0.13	0.14	0.27	0.04	0.05	0.09	0.11	0.35	0.46
0.08	0.23	0.31	0.35	0.49	0.84	0.08	0.16	0.24
0.12	0.37	0.49	0.14	0.13	0.27	0.08	0.10	0.18
0.07	0.06	0.13	0.47	0.41	0.88	0.11	0.34	0.45
0.05	0.05	0.10	0.04	0.07	0.11	0.06	0.31	0.37
0.03	0.03	0.06	0.05	0.08	0.13	0.34	0.43	0.77
0.05	0.11	0.16	0.06	0.09	0.15	0.07	0.54	0.61
0.08	0.08	0.16	0.04	0.10	0.14	0.79	0.67	1.46
0.02	0.06	0.08	0.32	0.18	0.50	0.69	0.17	0.86
0.07	0.14	0.21	0.06	0.17	0.23	0.08	0.15	0.23

silt	clay	couplet	silt	clay	couplet	silt	clay	couplet
0.22	0.45	0.67	0.13	0.14	0.27	0.04	0.09	0.13
0.04	0.30	0.34	0.10	0.20	0.30	0.07	0.18	0.25
0.05	0.26	0.31	0.29	0.29	0.58	0.19	0.39	0.58
0.33	0.48	0.81	0.29	0.21	0.50	0.08	0.28	0.36
0.06	1.17	1.23	0.04	0.09	0.13	0.09	0.09	0.18
0.11	0.10	0.21	0.06	0.25	0.31	0.94	0.39	1.33
0.55	0.27	0.82	0.29	0.28	0.57	0.55	0.51	1.06
0.07	0.34	0.41	0.10	0.23	0.33	0.05	0.08	0.13
0.07	0.27	0.34	0.04	0.11	0.15	0.07	0.08	0.15
0.23	0.23	0.46	1.32	0.80	2.12	0.08	0.17	0.25
0.07	0.37	0.44	0.66	0.11	0.77	0.07	0.07	0.14
0.08	0.09	0.17	0.26	0.26	0.52	0.10	0.39	0.49
0.38	0.21	0.59	0.31	0.31	0.62	0.23	0.11	0.34
0.03	0.61	0.64	0.04	0.05	0.09	0.62	0.21	0.83
0.14	0.31	0.45	0.04	0.09	0.13	0.07	0.18	0.25
0.04	0.25	0.29	0.05	0.16	0.21	0.07	0.05	0.12
0.04	0.17	0.21	0.07	0.20	0.27	0.06	0.25	0.31
0.25	0.45	0.70	0.05	0.55	0.60	0.06	0.45	0.51
0.27	0.13	0.40	0.35	0.31	0.66	0.03	0.21	0.24
0.04	0.11	0.15	0.19	0.45	0.64	0.10	0.15	0.25
0.13	0.50	0.63	0.04	0.21	0.25	0.50	0.57	1.07
0.28	0.46	0.74	0.12	0.16	0.28	0.06	0.14	0.20
0.12	0.22	0.34	0.14	0.16	0.30	0.04	0.08	0.12
0.07	0.10	0.17	0.11	0.23	0.34	0.12	0.39	0.51
0.28	0.48	0.76	0.05	0.13	0.18	0.61	0.13	0.74
0.41	0.26	0.67	0.10	0.28	0.38	0.04	0.37	0.41
0.03	0.05	0.08	0.28	0.34	0.62	0.04	0.16	0.20
0.25	0.33	0.58	0.06	0.31	0.37	0.12	0.08	0.20
0.28	0.21	0.49	0.04	0.07	0.11	0.12	0.08	0.20
0.14	0.17	0.31	0.14	0.32	0.46	0.04	0.44	0.48
0.21	0.17	0.38	0.08	0.06	0.14	0.08	0.10	0.18
0.10	0.38	0.48	0.07	0.30	0.37	0.07	0.09	0.16
0.13	0.07	0.20	0.23	0.17	0.40	0.10	0.08	0.18
0.08	0.28	0.56	0.14	0.18	0.32	0.06	0.11	0.17
0.12	0.10	0.22	0.05	0.17	0.22	0.17	0.08	0.25
0.09	0.37	0.46	0.63	0.18	0.81	0.16	0.41	0.57

silt	clay	couplet	silt	clay	couplet	silt	clay	couplet
0.05	0.11	0.16	0.04	0.12	0.16	0.23	0.06	0.29
0.28	0.19	0.47	0.10	0.28	0.38	0.05	0.31	0.36
0.08	0.10	0.18	0.15	0.52	0.67	0.32	0.11	0.43
0.04	0.11	0.15	0.48	0.28	0.76	0.38	0.09	0.47
0.07	0.14	0.21	0.04	0.07	0.11	0.14	0.12	0.26
0.09	0.31	0.40	0.03	0.11	0.14	0.07	0.08	0.15
0.21	0.22	0.43	0.13	0.23	0.36	0.08	0.11	0.19
0.09	0.09	0.18	0.16	0.11	0.27	0.10	0.08	0.18
0.07	0.13	0.20	0.05	0.20	0.25	0.11	0.09	0.20
0.07	0.10	0.17	0.04	0.12	0.16	0.04	0.18	0.22
0.06	0.21	0.27	0.11	0.29	0.40	0.04	0.18	0.22
0.77	0.23	1.00	0.26	0.08	0.34	0.05	0.05	0.10
0.08	0.08	0.16	0.09	0.20	0.29	0.04	0.04	0.08
0.07	0.20	0.27	0.06	0.16	0.22	0.09	0.09	0.18
0.10	0.39	0.49	0.06	0.17	0.23	0.05	0.19	0.24
0.46	0.37	0.83	0.09	0.06	0.15	0.03	0.13	0.16
0.04	0.18	0.22	0.10	0.08	0.18	0.11	0.14	0.25
0.11	0.20	0.31	0.05	0.17	0.22	0.06	0.12	0.18
0.21	0.42	0.63	0.06	0.10	0.16	0.18	0.25	0.43
0.13	0.10	0.23	0.16	0.09	0.25	0.06	0.11	0.17
0.07	0.16	0.23	0.07	0.06	0.13	0.08	0.13	0.21
0.17	0.38	0.55	0.28	0.25	0.53	0.40	0.13	0.53
0.30	0.18	0.48	0.16	0.22	0.38	0.04	0.08	0.12
0.21	0.18	0.39	0.05	0.40	0.45	0.05	0.11	0.16
0.07	0.28	0.35	0.08	0.13	0.21	0.37	0.13	0.50
0.15	0.09	0.24	0.32	0.14	0.46	0.05	0.33	0.38
0.08	0.19	0.27	0.03	0.12	0.15	0.07	0.37	0.44
0.09	0.19	0.28	0.08	0.34	0.42	0.11	0.10	0.21
0.30	0.52	0.82	0.13	0.07	0.20	0.19	0.10	0.29
0.05	0.17	0.22	0.05	0.10	0.15	0.05	0.22	0.27
0.05	0.32	0.37	0.09	0.10	0.19	0.18	0.17	0.35
1.30	0.16	1.46	0.04	0.17	0.21	0.04	0.10	0.14
0.11	0.12	0.23	0.35	0.18	0.53	0.06	0.26	0.32
0.10	0.08	0.18	0.05	0.06	0.11	0.08	0.05	0.13
0.06	0.06	0.12	0.04	0.14	0.18	0.19	0.13	0.32
0.05	0.09	0.14	0.04	0.08	0.12	0.05	0.04	0.09
0.04	0.09	0.13	0.10	0.44	0.54	0.63	0.51	1.14

silt	clay	couplet	silt	clay	couplet	silt	clay	couplet
0.08	0.30	0.38	0.28	0.24	0.52	0.06	0.32	0.38
0.06	0.08	0.14	0.08	0.11	0.19	0.38	0.26	0.64
0.20	0.15	0.35	0.20	0.10	0.30	0.07	0.24	0.31
0.06	0.05	0.11	0.07	0.17	0.24	0.08	0.07	0.15
0.12	0.15	0.27	0.05	0.09	0.14	0.04	0.19	0.23
0.10	0.22	0.32	0.09	0.06	0.15	0.14	0.13	0.27
0.03	0.04	0.07	0.04	0.06	0.10	0.07	0.33	0.40
0.10	0.47	0.57	0.03	0.03	0.06	0.35	0.10	0.45
0.05	0.04	0.09	0.07	0.09	0.16	0.04	0.15	0.19
0.12	0.19	0.31	0.10	0.14	0.24	0.04	0.16	0.20
0.12	0.06	0.18	0.05	0.23	0.28	0.18	0.20	0.38
0.04	0.04	0.08	0.04	0.05	0.09	0.28	0.10	0.38
0.09	0.13	0.22	0.04	0.11	0.15	0.09	0.06	0.15
0.03	0.09	0.12	0.03	0.05	0.08	0.07	0.18	0.25
0.04	0.17	0.21	0.04	0.30	0.34	0.26	0.21	0.47
0.06	0.09	0.15	0.14	0.12	0.26	0.14	0.23	0.37
0.78	0.31	1.09	0.11	0.09	0.20	0.27	0.23	0.50
0.05	0.04	0.09	0.07	0.06	0.13	0.71	0.35	1.06
0.08	0.35	0.43	0.06	0.12	0.18	0.08	0.12	0.20
0.07	0.04	0.11	0.10	0.11	0.21	0.07	0.04	0.11
0.04	0.08	0.12	0.09	0.06	0.15	0.34	0.15	0.49
0.08	0.10	0.18	0.22	0.34	0.56	0.03	0.14	0.17
0.04	0.11	0.15	0.56	0.23	0.79	0.08	0.04	0.12
0.72	0.34	1.06	0.26	0.25	0.51	0.24	0.15	0.39
0.07	0.19	0.26	0.06	0.30	0.36	0.23	0.37	0.60
0.12	0.13	0.25	0.18	0.06	0.24	0.05	0.23	0.28
0.40	0.26	0.66	0.05	0.04	0.09	0.32	0.18	0.50
0.13	0.10	0.23	0.04	0.07	0.11	0.09	0.14	0.23
0.09	0.17	0.26	0.03	0.08	0.11	0.09	0.06	0.15
0.09	0.08	0.17	0.15	0.07	0.22	0.09	0.06	0.15
0.08	0.05	0.13	0.06	0.07	0.13	0.07	0.10	0.17
0.39	0.11	0.50	0.45	0.09	0.54	0.15	0.15	0.30
0.07	0.25	0.32	0.10	0.31	0.41	0.11	0.13	0.24
0.04	0.31	0.35	0.23	0.13	0.36	0.09	0.08	0.17
0.08	0.42	0.50	0.06	0.15	0.21	0.09	0.10	0.19
0.10	0.04	0.14	0.31	0.11	0.42	0.16	0.08	0.24

silt	clay	couplet	silt	clay	couplet	silt	clay	couplet
0.18	0.19	0.37	0.06	0.18	0.24	0.08	0.06	0.14
0.06	0.13	0.19	0.13	0.15	0.28	0.05	0.03	0.08
0.04	0.03	0.07	0.05	0.10	0.15	0.08	0.19	0.27
0.06	0.16	0.22	0.07	0.05	0.12	0.08	0.16	0.24
0.30	0.06	0.36	0.21	0.10	0.31	0.15	0.08	0.23
0.35	0.19	0.54	0.42	0.20	0.62	0.05	0.03	0.08
0.09	0.51	0.60	0.07	0.23	0.30	0.08	0.12	0.20
0.36	0.26	0.62	0.10	0.10	0.20	0.10	0.13	0.23
0.05	0.23	0.28	0.06	0.14	0.20	0.08	0.34	0.42
0.04	0.23	0.27	0.11	0.12	0.23	0.65	0.15	0.80
0.05	0.09	0.14	0.08	0.28	0.36	0.30	0.06	0.36
0.05	0.19	0.24	0.06	0.09	0.15	0.05	0.09	0.14
0.04	0.05	0.09	0.25	0.15	0.40	0.10	0.25	0.35
0.23	0.05	0.28	0.30	0.05	0.35	0.88	0.33	1.21
0.34	0.10	0.44	0.07	0.03	0.10	0.06	0.48	0.54
0.15	0.16	0.31	0.08	0.15	0.23	0.06	0.22	0.28
0.19	0.45	0.64	0.18	0.13	0.31	0.05	0.02	0.07
0.14	0.26	0.40	0.97	0.10	1.07	0.30	0.28	0.58
0.08	0.08	0.16	0.05	0.32	0.37	0.08	0.26	0.34
0.06	0.06	0.12	0.10	0.25	0.35	0.11	0.08	0.19
0.10	0.14	0.24	0.33	0.11	0.44	0.05	0.03	0.08
0.10	0.05	0.15	0.05	0.12	0.17	0.07	0.07	0.14
0.12	0.09	0.21	0.05	0.16	0.21	0.38	0.21	0.59
0.30	0.15	0.45	0.07	0.11	0.18	0.11	0.14	0.25
0.26	0.17	0.43	0.07	0.04	0.11	0.06	0.04	0.10
0.04	0.07	0.11	0.05	0.21	0.26	0.05	0.06	0.11
0.05	0.12	0.17	0.23	0.05	0.28	0.09	0.08	0.17
0.32	0.05	0.37	0.08	0.13	0.21	0.06	0.11	0.17
0.23	0.24	0.47	0.48	0.12	0.60	0.24	0.61	0.85
0.43	0.21	0.64	0.06	0.06	0.12	0.14	0.05	0.19
0.26	0.12	0.38	0.12	0.15	0.27	0.09	0.08	0.17
0.09	0.18	0.27	0.09	0.07	0.16	0.47	0.10	0.57
0.24	0.15	0.39	0.07	0.31	0.38	0.05	0.07	0.12
0.15	0.45	0.60	0.36	0.08	0.44	0.38	0.31	0.69
0.46	0.06	0.52	0.04	0.06	0.10	0.06	0.09	0.15
0.10	0.35	0.45	0.05	0.03	0.08	0.06	0.03	0.09

silt	clay	couplet	silt	clay	couplet	silt	clay	couplet
0.10	0.07	0.17	0.07	0.05	0.12	0.23	0.47	0.70
0.26	0.08	0.34	0.05	0.04	0.09	0.10	0.36	0.46
0.11	0.07	0.18	0.06	0.30	0.36	0.22	0.25	0.47
0.04	0.04	0.08	0.04	0.08	0.12	0.09	0.42	0.51
0.04	0.08	0.12	0.04	0.08	0.12	0.06	0.28	0.34
0.07	0.13	0.20	0.06	0.06	0.12	0.30	0.17	0.47
0.06	0.13	0.19	0.05	0.06	0.11	0.08	0.09	0.17
0.65	0.48	1.13	0.62	0.10	0.72	0.20	0.10	0.30
0.07	0.07	0.14	0.23	0.04	0.27	0.08	0.08	0.16
0.35	0.33	0.68	0.05	0.18	0.23	0.05	0.05	0.10
0.20	0.17	0.37	0.20	0.12	0.32	0.05	0.02	0.07
0.10	0.17	0.27	0.15	0.25	0.40	0.10	0.23	0.33
0.08	0.05	0.13	0.25	0.18	0.43	0.27	0.35	0.62
0.10	0.10	0.20	0.11	0.11	0.22	0.16	0.10	0.26
0.19	0.17	0.36	0.04	0.08	0.12	0.05	0.03	0.08
0.05	0.37	0.42	0.05	0.04	0.09	0.10	0.07	0.17
0.09	0.24	0.33	0.11	0.09	0.20	0.09	0.05	0.14
0.45	0.16	0.61	0.05	0.25	0.30	0.05	0.07	0.12
0.08	0.18	0.26	0.24	0.08	0.32	0.08	0.05	0.13
0.04	0.13	0.17	0.04	0.28	0.32	0.08	0.08	0.16
0.05	0.07	0.12	0.07	0.26	0.33	0.07	0.17	0.24
0.15	0.42	0.57	0.13	0.06	0.19	0.15	0.23	0.38
0.06	0.05	0.11	0.06	0.04	0.10	0.07	0.11	0.18
0.09	0.17	0.26	0.04	0.09	0.13	0.13	0.10	0.23
0.28	0.27	0.55	0.06	0.12	0.18	0.25	0.10	0.35
0.27	0.21	0.48	0.04	0.10	0.14	0.04	0.28	0.32
0.09	0.14	0.23	0.05	0.08	0.13	0.25	0.12	0.37
0.21	0.29	0.50	0.07	0.12	0.19	0.03	0.17	0.20
0.09	0.24	0.33	0.08	0.32	0.40	0.03	0.06	0.09
0.07	0.08	0.15	0.93	0.09	1.02	0.06	0.04	0.10
0.05	0.07	0.12	0.08	0.09	0.17	0.17	0.17	0.34
0.11	0.20	0.31	0.06	0.05	0.11	0.05	0.28	0.33
0.06	0.07	0.13	0.05	0.17	0.22	0.07	0.07	0.14
0.16	0.14	0.30	0.04	0.08	0.12	0.08	0.23	0.31
0.05	0.13	0.18	0.22	0.33	0.55	0.05	0.06	0.11

silt	clay	couplet	silt	clay	couplet	silt	clay	couplet
0.05	0.13	0.18	0.04	0.08	0.12	0.08	0.23	0.31
0.06	0.13	0.19	0.22	0.33	0.55	0.05	0.06	0.11
0.13	0.11	0.24	0.23	0.47	0.70	0.05	0.13	0.18
0.07	0.03	0.10	0.10	0.36	0.46	0.06	0.13	0.19
0.05	0.23	0.28	0.22	0.25	0.47	0.13	0.11	0.24
0.07	0.06	0.13	0.09	0.42	0.51	0.07	0.03	0.10
0.14	0.27	0.41	0.06	0.28	0.34	0.05	0.23	0.28
0.22	0.16	0.38	0.30	0.17	0.47	0.07	0.06	0.13
0.10	0.06	0.16	0.08	0.09	0.17	0.14	0.27	0.41
0.15	0.10	0.25	0.20	0.10	0.30	0.22	0.16	0.38
0.23	0.04	0.27	0.08	0.08	0.16	0.10	0.06	0.16
0.05	0.18	0.23	0.05	0.05	0.10	0.15	0.03	0.18
0.20	0.12	0.32	0.04	0.03	0.07	0.11	0.11	0.22
0.15	0.25	0.40	0.10	0.23	0.33	0.04	0.10	0.14
0.25	0.18	0.43	0.27	0.35	0.62	0.06	0.25	0.31
0.11	0.11	0.22	0.16	0.10	0.26	0.36	0.11	0.47
0.04	0.08	0.12	0.05	0.03	0.08	0.06	0.15	0.21
0.05	0.04	0.09	0.10	0.07	0.17	0.08	0.09	0.17
0.11	0.09	0.20	0.09	0.05	0.14	0.04	0.20	0.24
0.05	0.25	0.30	0.05	0.07	0.12	0.04	0.05	0.09
0.24	0.08	0.32	0.08	0.05	0.13	0.08	0.10	0.18
0.04	0.28	0.32	0.08	0.08	0.16	0.08	0.18	0.26
0.07	0.26	0.33	0.06	0.18	0.24	0.25	0.18	0.43
0.13	0.06	0.19	0.15	0.23	0.38	0.07	0.11	0.18
0.06	0.04	0.10	0.07	0.11	0.18	0.05	0.05	0.10
0.04	0.09	0.13	0.13	0.10	0.23	0.04	0.16	0.20
0.06	0.12	0.18	0.25	0.10	0.35	0.50	0.18	0.68
0.05	0.09	0.14	0.04	0.28	0.32	0.10	0.10	0.20
0.05	0.08	0.13	0.25	0.12	0.37	0.05	0.16	0.21
0.07	0.12	0.19	0.03	0.17	0.20	0.07	0.33	0.40
0.08	0.32	0.40	0.03	0.07	0.10	0.04	0.25	0.29
0.93	0.09	1.02	0.06	0.04	0.10	0.19	0.14	0.33
0.08	0.09	0.17	0.17	0.17	0.34	0.05	0.06	0.11
0.06	0.05	0.11	0.05	0.28	0.33	0.06	0.15	0.21
0.05	0.17	0.22	0.07	0.07	0.14	0.26	0.18	0.44

silt	clay	couplet	silt	clay	couplet	silt	clay	couplet
0.10	0.05	0.15	0.10	0.06	0.16	0.05	0.05	0.10
0.05	0.06	0.11	0.11	0.15	0.26	0.06	0.05	0.11
0.05	0.21	0.26	0.18	0.15	0.33	0.07	0.04	0.11
0.08	0.21	0.29	0.11	0.13	0.24	0.10	0.24	0.34
0.14	0.13	0.27	0.07	0.04	0.11	0.18	0.12	0.30
0.07	0.05	0.12	0.14	0.08	0.22	0.10	0.21	0.31
0.12	0.20	0.32	0.08	0.31	0.39	0.20	0.24	0.44
0.17	0.20	0.37	0.19	0.35	0.54	0.05	0.40	0.45
0.08	0.12	0.20	0.38	0.06	0.44	0.07	0.11	0.18
0.22	0.07	0.29	0.40	0.24	0.64	0.08	0.07	0.15
0.08	0.10	0.18	0.06	0.10	0.16	0.44	0.17	0.61
0.09	0.04	0.13	0.06	0.17	0.23	0.14	0.15	0.29
0.28	0.03	0.31	0.05	0.14	0.19	0.15	0.05	0.20
0.24	0.09	0.33	0.54	0.15	0.69	0.10	0.32	0.42
0.13	0.21	0.34	0.06	0.46	0.52	0.06	0.09	0.15
0.07	0.08	0.15	0.07	0.14	0.21	0.11	0.14	0.25
0.05	0.27	0.32	0.10	0.06	0.16			
0.25	0.08	0.33	0.16	0.38	0.54			
0.16	0.12	0.28	0.08	0.25	0.33			
0.10	0.04	0.14	0.12	0.13	0.25			
0.12	0.22	0.34	0.08	0.20	0.28			
0.28	0.06	0.34	0.09	0.47	0.56			
0.09	0.25	0.34	0.10	0.05	0.15			
0.04	0.32	0.36	0.08	0.04	0.12			
0.10	0.28	0.38	0.06	0.77	0.83			
0.28	0.10	0.38	0.60	0.38	0.98			
0.11	0.06	0.17	0.10	0.08	0.18			
0.11	0.57	0.68	0.06	0.46	0.52			
0.26	0.09	0.35	0.12	0.68	0.80			
0.12	0.45	0.57	0.23	0.87	1.10			
0.20	0.24	0.44	0.72	0.48	1.20			
0.10	0.17	0.27	0.14	0.18	0.32			
0.16	0.40	0.56	0.16	0.17	0.33			
0.06	0.12	0.18	0.05	0.06	0.11			
0.41	0.18	0.59	0.04	0.05	0.09			
0.10	0.20	0.30	0.05	0.05	0.10			

APPENDIX V

Silt, clay, and total couplet thickness (in feet) of the railroad-cut section of the Haymond Formation.

silt	clay	couplet	silt	clay	couplet	silt	clay	couplet
1.67	0.11	1.78	0.13	0.06	0.19	0.07	0.07	0.14
0.19	0.09	0.28	0.14	0.05	0.19	0.05	0.16	0.21
0.12	0.10	0.22	0.08	0.13	0.21	0.02	0.14	0.16
0.05	0.07	0.12	0.05	0.06	0.11	0.26	0.03	0.29
0.09	0.07	0.16	0.05	0.13	0.18	0.07	0.09	0.16
0.04	0.13	0.17	0.23	0.04	0.27	0.04	0.07	0.11
0.06	0.19	0.25	0.11	0.09	0.20	0.02	0.03	0.05
0.16	0.09	0.25	0.32	0.07	0.39	0.03	0.14	0.17
0.02	0.22	0.24	0.03	0.06	0.09	0.41	0.13	0.54
0.22	0.56	0.78	0.10	0.08	0.19	0.64	0.04	0.68
0.04	0.08	0.12	0.21	0.17	0.38	0.21	0.10	0.31
0.65	0.20	0.85	0.02	0.05	0.07	0.09	0.11	0.20
0.07	0.06	0.13	0.08	0.17	0.25	0.10	0.19	0.29
0.05	0.12	0.17	0.02	0.05	0.07	0.15	0.80	0.95
0.04	0.04	0.08	0.03	0.07	0.10	0.15	0.11	0.26
0.15	0.05	0.20	0.03	0.04	0.07	0.05	0.10	0.14
0.05	0.06	0.11	0.03	0.05	0.08	0.04	0.08	0.12
0.02	0.09	0.11	0.11	0.04	0.15	0.04	0.07	0.11
0.18	0.05	0.23	0.06	0.08	0.14	0.02	0.10	0.12
0.04	0.24	0.28	0.46	0.06	0.52	0.10	0.03	0.13
0.02	0.05	0.07	0.02	0.05	0.07	0.04	0.05	0.09
0.06	0.22	0.28	0.04	0.18	0.22	0.12	0.09	0.21
0.14	0.26	0.40	0.10	0.40	0.50	0.05	0.09	0.14
0.03	0.20	0.23	0.02	0.10	0.12	0.06	0.17	0.23
0.32	0.05	0.37	0.15	0.07	0.22	0.03	0.12	0.15
0.15	0.20	0.35	0.07	0.13	0.20	0.12	0.14	0.26
0.09	0.23	0.32	0.13	0.08	0.21	0.10	0.18	0.28
0.07	0.24	0.31	0.06	0.23	0.29	0.23	0.07	0.30
0.08	0.27	0.35	0.46	0.21	0.67	0.02	0.18	0.20

silt	clay	couplet
0.10	0.12	0.22
0.14	0.19	0.33
0.50	0.07	0.57
0.05	0.12	0.17
0.07	0.07	0.14
0.03	0.07	0.10
0.49	0.19	0.68
0.09	0.22	0.31
0.02	0.12	0.14
0.02	0.11	0.13
0.09	0.47	0.56
0.14	0.14	0.28
0.24	0.08	0.32
0.08	0.11	0.19
0.02	0.10	0.12
0.02	0.09	0.11
0.21	0.08	0.29
0.03	0.10	0.13
0.10	0.12	0.22
0.09	0.09	0.18
0.05	0.20	0.25
0.10	0.04	0.14
0.24	0.16	0.40
0.07	0.07	0.14
0.15	0.25	0.40
0.02	0.05	0.07
0.04	0.08	0.12
0.02	0.03	0.05
0.05	0.12	0.17

APPENDIX VI

Summary of the number of years between storms producing a sea level anomaly greater than 2 feet for 17 U. S. Coast and Geodetic Survey tide stations on the Atlantic and Gulf coasts (data *from* Harris, 1963).

Station	Number of years between storms	Regional means
North Atlantic:		3.87
Eastport	4.36	
Portland	6.81	
Boston	3.45	
Newport	2.60	
Battery	2.11	
Atlantic City	1.71	
South Atlantic:		1.57
Hampton Roads	1.68	
Southport	1.47	
Charleston	1.33	
Mayport	1.30	
Miami	1.96	
Gulf coast:		2.41
Key West	2.30	
Tampa	1.52	
Ceder Keys	1.60	
Pensacola	2.57	
Galveston	2.84	
Port Isabel	3.60	